Geomorphology 484 (2025) 109854

Contents lists available at ScienceDirect

Geomorphology

journal homepage: www.journals.elsevier.com/geomorphology

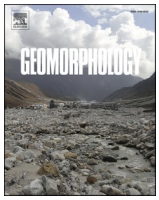

Landsystem models from remote and field based geomorphological mapping reveal diverse glacier dynamics on Svalbard

Rebecca McCerery [a,*], Bethan J. Davies [b], Harold Lovell [c], Rosalia Calvo-Ryan [d], David A. Pearce [d,e], Jakub Małecki [f], John Woodward [a]

[a] Department of Geography and Environmental Science, Northumbria University, Newcastle Upon Tyne NE1 8ST, United Kingdom
[b] School of Geography, Politics and Sociology, Newcastle University, Newcastle Upon Tyne NE1 7RU, United Kingdom
[c] School of the Environment and Life Sciences, University of Portsmouth, Portsmouth PO1 2UP, United Kingdom
[d] Department of Health and Life Sciences, Northumbria University, Newcastle Upon Tyne NE1 8ST, United Kingdom
[e] British Antarctic Survey, High Cross, Madingley Road, Cambridge CB3 0ET, United Kingdom
[f] Institute of Geoecology and Geoinformation, Adam Mickiewicz University, Poznań 61-680, Poland

ARTICLE INFO

Keywords:
Thermal regimes
Svalbard
Arctic
Glacial landsystems

ABSTRACT

Glacial landsystems are geomorphological records produced by glaciers that provide important insights into past and present glacier dynamics. Here, we present a snapshot of the diversity in glacier landsystems in Svalbard. We present remote and field geomorphological mapping from 11 glaciers: seven in south Spitsbergen (Scottbreen, Renardbreen, Antoniabreen, Penckbreen, Bakaninbreen, Paulabreen and Skobreen) and four in northwest Spitsbergen (Charlesbreen, Protektorbreen, Bullbreen, and Ferdinandbreen). These examples include landform assemblages that (1) are diagnostic of recent surging in terrestrial and marine settings; (2) are characteristic of thinning polythermal glaciers that have previously been more dynamic; and (3) represent rapidly vanishing glaciers, the geomorphological endpoint for Svalbard glaciers characterised by the fragmentation and down-wasting of small cold-based glaciers. We synthesize these into four landsystem models to provide a framework for interpreting glacier dynamics in Svalbard based on geomorphological records. The hypsometries of many land-terminating glaciers in Svalbard suggests that we will increasingly observe the transition from polythermal to cold-based glacier thermal regimes as the climate continues to warm, ultimately leading to more vanishing glaciers. This has important wider implications for changing water, sediment and biogeochemical fluxes which will impact subglacial, forefield and ocean ecosystems.

1. Introduction

The High Arctic Svalbard archipelago is covered by icefields and marine- and land-terminating glaciers, comprising ~57 % of land area and representing a substantial glacierised area vulnerable to climate change (Nuth et al., 2013). Most glaciers are rapidly thinning as the Arctic warms, with an estimated ~8 Gt yr^{-1} lost between 1936 and ~ 2010 (Geyman et al., 2022) and a further 16 Gt yr^{-1} between 2011 and 2017 (Morris et al., 2020). This thinning is impacting glacier configurations and thermal regimes, including examples of marine-terminating glaciers retreating on to land (e.g. Błaszczyk et al., 2009; van Pelt et al., 2012; Holmlund, 2021; Zagórski et al., 2023) and polythermal glaciers, which contain areas of temperate ice at the pressure melting point, transitioning to cold-based glaciers that are then frozen to the substrate (e.g. Bælum and Benn, 2011; Mannerfelt et al., 2024a). For many smaller land-terminating glaciers, this thinning is increasingly leading to instances of glacier fragmentation and disconnection from larger accumulation areas, ultimately resulting in the cessation of glacier flow other than by the slow internal deformation of the ice column. Disconnected and stagnating glaciers represent the likely end stage of many of Svalbard's smaller glaciers under the current pace of recession (Małecki, 2016).

At the opposite end of the scale in terms of glacier dynamics, many Svalbard glaciers are known to surge (Sevestre and Benn, 2015) and are continuing to do so even as glaciers are thinning in a warming climate (e.g. Kääb et al., 2023; Mannerfelt et al., 2024b). During surges, ice velocities increase dramatically for several years, often combined with a period of frontal advance, before reverting to slow flow and recession during a quiescent phase lasting anywhere from decades to centuries (e.g. Dowdeswell et al., 1991; Hagen et al., 1993; Murray et al., 2003).

* Corresponding author.

https://doi.org/10.1016/j.geomorph.2025.109854
Received 31 March 2025; Received in revised form 21 May 2025; Accepted 21 May 2025
Available online 24 May 2025

Surge-type glaciers are particularly vulnerable to climate change, experiencing enhanced mass loss compared to non-surge-type glaciers (e.g. Yde and Knudsen, 2007; Kochtitzky and Copland, 2022).

This diverse range in dynamics exhibited by Svalbard glaciers, from surge-type glaciers to small cold-based glaciers that are thinning and fragmenting, makes it an excellent natural laboratory for deciphering the impact of climate change on different types of glaciers and helps to place present glacier conditions in the context of past behaviour. However, longer-term observations of glacier change are typically limited to the satellite remote sensing era (since ~1970). An alternative and potentially very rich source of information on glacier change can be found in the geomorphological records they produce. Glacial landsystem models are an established technique for understanding past and present glacier dynamics using sediment-landform assemblages and have been successfully applied in glacierised regions across the world (e.g. Krüger, 1994; Evans and Twigg, 2002; Krüger et al., 2010; Davies et al., 2013; Benn et al., 2014; Evans, 2014; Evans and Rea, 2014; Jónsson et al., 2014; Schomacker et al., 2014; Ingólfsson et al., 2016; Kjær et al., 2008; Małecki et al., 2018; Chandler et al., 2020). The glacial landsystem approach aims to group suites of sediment-landform assemblages into broad categories based on the genetic linkages of their process-form signature (e.g. Clayton and Moran, 1974; Evans and Rea, 1999; Evans and Twigg, 2002; Evans, 2014).

Previous work on glacier landsystems in Svalbard has identified characteristic landform assemblages associated with land- and marine-terminating surge-type glaciers (e.g. Boulton, 1972; Boulton et al., 1999; Christoffersen et al., 2005; Ottesen and Dowdeswell, 2006; Schomacker and Kjær, 2008; Ottesen et al., 2008, Ottesen et al., 2017; Flink et al., 2015; Farnsworth et al., 2016; Lovell and Boston, 2017; Aradóttir et al., 2019) and polythermal valley glaciers (e.g. Glasser and Hambrey, 2005; Ewertowski, 2014; Ewertowski et al., 2019; Ewertowski and Tomczyk, 2020). Common features reported in Svalbard surge landsystems are crevasse-squeeze ridges (CSRs), glacial lineations, flutes, eskers and glaciotectonic moraines. CSRs are formed when saturated subglacial debris is injected into a glacier base fractured by longitudinal stretching associated with enhanced ice flow during the surge, before being deposited and preserved during quiescent phase ice stagnation (Sharp, 1988; Rea and Evans, 2011; Lovell et al., 2015). Increased ice velocities also contribute to the formation of streamlined glacial lineations and flutes (e.g. Christoffersen et al., 2005; Ottesen and Dowdeswell, 2006). High basal water pressures can lead to meltwater occupying basal fracture networks, producing zig-zag eskers (e.g. Evans et al., 2022) in addition to traditional sinuous eskers (e.g. Ottesen et al., 2008, Ottesen et al., 2017). Glaciotectonic moraines mark the maximum extent of surge advances where proglacial deformation of glacial, fluvial, lacustrine and marine sediments (Hart and Watts, 1997; Boulton et al., 1999; van der Meer, 2004; Kristensen et al., 2009; Lønne, 2016; Lovell and Boston, 2017), with low-angle debris-flow lobes typically emanating from their distal flanks in submarine settings (e.g. Ottesen and Dowdeswell, 2006; Ottesen et al., 2008; Ottesen et al., 2017; Flink et al., 2015). Stagnation and frontal recession during quiescence can also produce extensive areas of stagnation terrain (e.g. Lovell et al., 2018a) and minor retreat moraines found on the seafloor (e.g. Ottesen and Dowdeswell, 2006; Flink et al., 2015).

Landsystems based on polythermal valley glaciers also contain ice stagnation terrain as a key component (Glasser and Hambrey, 2005; Ewertowski and Tomczyk, 2020). This terrain is typically enclosed by an ice-cored latero-frontal moraine system, which may be partly or completely censored by glaciofluvial activity, with outwash plains extending beyond the moraines. The inner zone of the Glasser and Hambrey (2005) polythermal valley glacier landsystem is characterised by a till plain covered by streamlined landforms and supraglacial debris stripes (linear sediment stripes in a proglacial position that originated supraglacially, i.e. from medial moraines), interrupted by significant fluvial reworking. Proglacial icings surrounding the main meltwater drainage have been suggested as evidence for polythermal conditions (e.g. Hagen et al., 2003), although this association has been questioned (Mallinson et al., 2019). It is important to note that since the Glasser and Hambrey (2005) model was presented, many polythermal valley glaciers have continued to thin and downwaste, leading to an evolving landsystem (e.g. Ewertowski, 2014).

In this study, we aim to outline a continuum of glacial landsystems on Svalbard, to characterise the diversity of terrestrial glacial landsystems on Svalbard, as well as understand the potential fate of glaciers on the archipelago under continued warming conditions. To address this aim we visited 11 different glaciers in south and northwest Spitsbergen, covering a variety of thermal regimes and a diversity of geomorphological signatures. We synthesize their geomorphological records into four new glacier landsystems, characterising a continuum of glacial behaviour from most to least dynamic: (1) marine-terminating and (2) land-terminating surge-type glacier landsystems; (3) an updated polythermal valley glacier landsystem; and (4) a first landsystem for small, vanishing cold-based glaciers in Svalbard. The latter in particular provides a valuable blueprint for understanding the potential fate of many small glaciers on the archipelago under continued warming conditions.

2. Study area

Svalbard is located between 74° and 81° N and has a High Arctic climate with a maritime influence (Drange et al., 2005, Farnsworth et al., 2020). The climate is characterised by low winter temperatures that persist for most of the year, supporting permafrost and snowy conditions (French, 2007; Eckerstorfer and Christiansen, 2011). However, the enhanced rate of warming observed in the Arctic, known as Arctic amplification (e.g. England et al., 2021), is most pronounced in Svalbard (Descamps et al., 2017). The archipelago has experienced temperature increase rates of 1.7 °C per decade, more than double the Arctic average and seven times the global average since 1991 (Nordli et al., 2020). This is in part due to its proximity to the North Atlantic warming current, which has been enhanced in recent decades (Ding et al., 2018).

Warmer and wetter winter conditions are resulting in an increase in rain-on-snow (ROS) events, which affect snow cover characteristics, enhance runoff, and drive current glacier mass loss (Geyman et al., 2022; Vickers et al., 2022). It is predicted that future glacier thinning rates will more than double those observed between 1936 and 2010 (Geyman et al., 2022). This contrasts dramatically to the condition of glaciers in the Little Ice Age (LIA) at the turn of the 19th and 20th centuries, when most Svalbard glaciers advanced to their maximum late-Holocene extent (Martín-Moreno et al., 2017).

We focus on 11 glaciers in south and northwest Spitsbergen (Fig. 1). Detailed geomorphological maps of each glacier can be found in McCerery et al. (2024). Table 1 provides key glaciological parameters for each glacier derived from the Randolph Glacier Inventory version 7 (RGI 7.0 Consortium, 2023), which has an approximate census date of 2000. Glacier hypsometry describes the distribution of a glacier's surface area over elevation (Furbish and Andrews, 1984) and is a quick measure of a glacier's condition at a fixed point in time. Elevation data from RGI 7.0 can be used to calculate a glacier's hypsometric index (HI) using the following equation from Jiskoot et al. (2009) and McGrath et al. (2017):

$$\mathrm{HI} = \frac{\mathrm{Zmax} - \mathrm{Zmed}}{\mathrm{Zmed} - \mathrm{Zmin}}, \text{if } 0 < HI < 1, \text{then HI} = \frac{-1}{\mathrm{HI}} \quad (1)$$

The HI categorises glaciers as: very top heavy (HI < −1.5), top heavy (−1.5 < HI < −1.2), equidimensional (−1.2 < HI < 1.2), bottom heavy (1.2 < HI < 1.5) and very bottom heavy (HI > 1.5).

2.1. Glaciers

The Bakaninbreen-Paulbreen marine-terminating glacier system is found at the head of Rindersbukta, the southern arm of Van

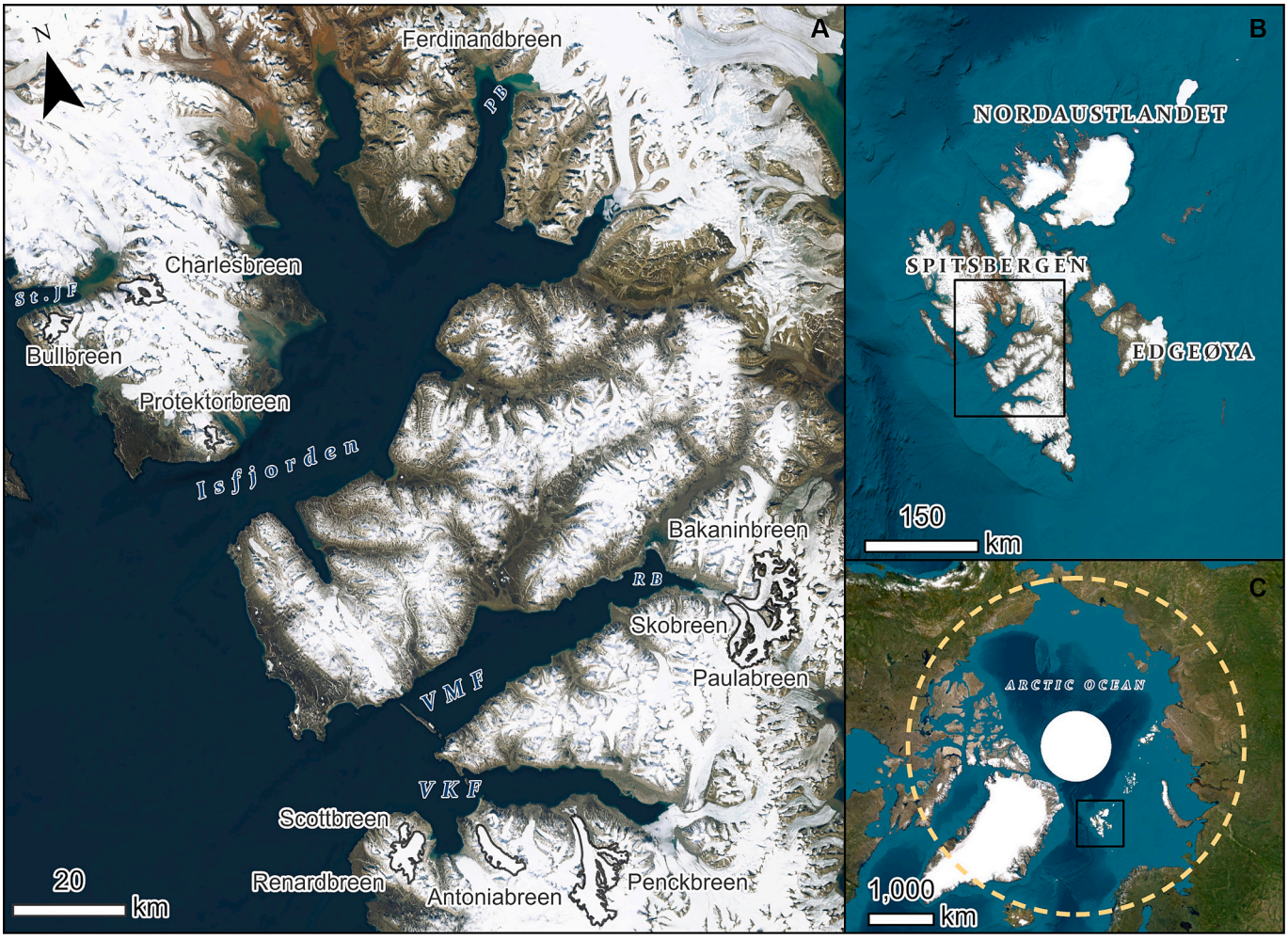

Fig. 1. (A) Locations of the 11 study glaciers in south and northwest Spitsbergen. PB – Petuniabukta, RB – Rindersbukta, St. JF – St. Jonsfjorden, VKF - Van Keulenfjorden, VMF – Van Mijenfjorden. The glacier outlines are from RGI 7.0. The black boxes in (B) and (C) depict the regional context of the study glaciers within the Svalbard archipelago and the Arctic circle (yellow dashed at 67° N). Background imagery is ESRI Basemap World Imagery.

Table 1
Summary of the key glaciological parameters (as reported in RGI 7.0) of the 11 glaciers investigated. Hypsometric Index (HI) categories: EQ = equidimensional, BH = bottom heavy, VBH = very bottom heavy.

Glacier name	Location	Length (km)	Total glacier area (km^2)	Average slope (°)	Aspect (°)	Minimum elevation (Z_{min})	Maximum elevation (Z_{max})	Median elevation (Z_{med})	Hypsometric Index (HI)
Paulabreen	77°42′ N 17°24′ E	15.4	60.1	9.3	342	91	821	401	1.4 (BH)
Bakaninbreen	77°45′ N 17°16′ E	15.9	56.0	9.5	269	140	790	428	1.3 (BH)
Skobreen	77°42’ N 17°03′ E	12.1	18.8	14.8	7	150	840	383	2.0 (VBH)
Penckbreen	77°28′ N 15°37′ E	22.2	80.4	8.3	6	171	1604	484	1.9 (VBH)
Renardbreen	77°31′ N 14°25′ E	10.4	30.6	11	46	133	694	380	1.3 (BH)
Charlesbreen	78°31’ N, 13°16′ E	10.1	25.7	10.6	324	66	795	324	1.1 (EQ)
Antoniabreen	77°30′ N 14°56′ E	12.8	27.1	9.1	358	160	889	490	1.2 (BH)
Scottbreen	77°32′ N 14°21′ E	4.0	4.7	12	38	199	657	379	1.5 (VBH)
Bullbreen	78°28’ N 12°40′ E	6.3	14.5	9.3	26	54	574	282	1.3 (BH)
Protektorbreen	78°15′ N 13°43′ E	4.4	6.8	13	56	43	746	223	2.7 (VBH)
Ferdinandbreen	78°40′ N 16°22′ E	2.2	1.3	15.8	75	298	696	479	1.2 (BH)

Mijenfjorden, and consists of the three main glaciers Bakaninbreen, Paulabreen and Skobreen (Fig. 1). The surge history of the Bakaninbreen-Paulabreen glacier system is well documented (Ottesen et al., 2008; Larsen et al., 2018; Lovell et al., 2018a). Paulabreen is currently the main marine-terminating glacier in Rindersbukta and is contiguous with land-terminating Bakaninbreen to the north and the tributary glacier Skobreen to the south. The HI for Bakaninbreen and Paulabreen fall within the bottom-heavy category, whereas Skobreen is very bottom-heavy (Table 1).

The combined Bakaninbreen-Paulabreen glacier system surged along the length of Rindersbukta and into Van Mijenfjorden at least four times from ~1300 to ~1898 (Hald et al., 2001; Kristensen et al., 2009). Within the current configuration of the glacier system, Bakaninbreen and Paulabreen are adjacent flow-units that surge independently and Skobreen is a surging tributary of Paulabreen (Sund, 2006; Benn et al., 2009). Bakaninbreen last surged in 1985–1995, with the surge terminating before it reached the terminus (Murray et al., 1998). A subsequent surge in the system occurred in 2003–2005, initiating in Skobreen and propagating into the lower trunk of the Paulabreen flow-unit. Paulabreen advanced ~2 km into Rindersbukta and laterally displaced Bakaninbreen to become the main component of the calving front (Kristensen and Benn, 2012; Lovell and Fleming, 2023). Since 2016, a surge front has been propagating down-glacier in the Paulabreen flow-unit, triggering a frontal advance in late 2024 (Mannerfelt et al., 2024b).

Penckbreen is a land-terminating surge-type glacier located in Van Keulenfjorden that partially terminates in a large proglacial lake (Fig. 1). Penckbreen's HI is very bottom-heavy. Prior to a recent surge in 2016–2020 (Koch et al., 2023; Mannerfelt et al., 2024b), Penckbreen formed a large glaciotectonic moraine complex, either during a surge event likely sometime in the early 19th century (Hart and Watts, 1997) or as a composite feature during two separate advances (Lønne, 2016).

Antoniabreen is a land-terminating valley glacier located at the mouth of Van Keulenfjorden (Fig. 1) that is classified as non-surge-type in the RGI 7.0 and has a bottom-heavy HI (Table 1). The glacier is enclosed by a latero-frontal moraine complex and separated from the fjord by a large outwash plain (McCerery et al., 2024).

Renardbreen is a land-terminating glacier in Recherchefjorden, adjacent to Van Keulenfjorden in south Spitsbergen and has a bottom-heavy HI (Fig. 1; Table 1). The glacier was marine-terminating up until the early 1990s and may have experienced surge events in the past (Zagórski et al., 2023). However this has not been directly observed and the glacier is classified as non-surge-type in the RGI 7.0.

Scottbreen is a small land-terminating glacier with a bottom-heavy HI located at the mouth of Recherchefjorden, neighbouring Renardbreen (Fig. 1). Its large outermost moraines were deposited during the late Holocene at ~1.7 ka (Philipps et al., 2017) and the glacier reached a similar position in the LIA following a reported surge (Hagen et al., 1993). Scottbreen's LIA maximum extent is suggested to have been larger than its size during the Younger Dryas (Mangerud and Landvik, 2007). Scottbreen's glacier area decreased by ~23 % between 1936 and 2012 (Zagórski et al., 2012), including a ~ 10 % reduction between 1986 and 2001 (Krawczyk and Bartoszewski, 2008).

Bullbreen is a land-terminating glacier located towards the mouth of St. Jonsfjorden (Fig. 1) with a bottom-heavy HI (Table 1). Trimlines and moraine areas extending to the fjord edge indicate the glacier was marine-terminating during the LIA (Farnsworth et al., 2017; Rootes and Clark, 2022). Bullbreen is classified as non-surge type in the RGI 7.0, but CSRs have been mapped recently in the forefield by McCerery et al. (2024).

Charlesbreen in St. Jonsfjorden is land-terminating and connected to a larger plateau icefield (Fig. 1). It is currently classified as non-surge type in the RGI 7.0, but CSRs have been mapped in the forefield previously (Farnsworth et al., 2017). Seafloor moraine ridges and trimlines extending downvalley to the fjord indicate that the glacier was likely marine-terminating during the LIA (Farnsworth et al., 2017; Rootes and Clark, 2022). The HI reveals Charlesbreen is equidimensional (Table 1).

Protektorbreen is a land-terminating cirque glacier located in Trygghamna at the mouth of Isfjorden (Fig. 1) and has a very bottom-heavy HI (Table 1). The extension of its moraine area to the fjord edge indicates that Protektorbreen historically terminated in Trygghamna as part of a combined glacier with neighbouring Harrietbreen and Kjerulfbreen. It is currently assumed to be thin and cold-based (Aradóttir et al., 2019).

Ferdinandbreen is the northernmost and smallest of the glaciers investigated, located in Petuniabukta at the northern end of Billefjorden (Fig. 1). Ferdinandbreen's HI is bottom-heavy (Table 1). The glacier is estimated to have lost approximately 43.9 % of its clean ice area since the LIA (Rachlewicz et al., 2007) and is currently likely to be cold-based (Małecki, 2013), but was probably polythermal when it was thicker and more extensive during the LIA.

3. Methods

Geomorphological mapping from remote sensing data was conducted in ArcGIS Pro (v3.1.1) using the ESRI Basemap World Imagery (1 m or above spatial resolution) following the protocols outlined in Chandler et al. (2018). Digital elevation models (DEMs; 2 m spatial resolution) were sourced from ArcticDEM Version 4.1 (Porter et al., 2023). Hillshade, aspect and slope models were derived from the DEM data and aided the interpretation of glaciological features and landforms. All landforms and glacier margins were digitally mapped at a scale of 1:5000. Field mapping took place in August and September 2022 for all glaciers except Ferdinandbreen, which was visited in August and September 2016. Field mapping primarily focused on ground-truthing remote mapping and the collection of uncrewed aerial vehicle (UAV) surveys of focus areas of the glacier forefields using a DJI Mavic Mini 2. UAV surveys were conducted at a flight altitude of 30 m and a camera tilt angle of 70°. DEMs and orthomosaics were created using structure from motion techniques in Agisoft software as per the methodologies outlined in Ely et al. (2017) and James et al. (2019). Mapping from all approaches was compiled in ArcGIS Pro and further details can be found in McCerery et al. (2024). Here, we also include published mapping of the seafloor geomorphology in Rindersbukta by Ottesen et al. (2008) to provide both the terrestrial and submarine components of the landsystems associated with the marine-terminating Bakaninbreen-Paulabreen glacier system.

4. Results

4.1. Individual Glaciers

4.1.1. Bakaninbreen-Paulabreen glacier system

Both sides of innermost Rindersbukta fjord are bound by well-developed lateral moraine areas cut by inactive meltwater channels. The distal parts of the moraine areas are characterised by frequent kettle lakes, particularly on the northern side of the fjord. At the Bakaninbreen margin, also on the northern side of the fjord, thick sequences of flat streamlined till plain are cut through by a large subglacial conduit, which has created a 10–20 m deep canyon with buried ice exposed at its base. CSRs are found in the moraine area on the northern side of the fjord as well as immediately in front of Bakaninbreen (Fig. 2C). CSRs closest to the glacier front are sharp and rectilinear, whereas those in more distal positions along the northern side of innermost Rindersbukta are generally smaller and less common. Ottesen et al. (2008) also mapped CSRs on the fjord floor close to the limits of our terrestrial mapping. A large sinuous esker approximately 700 m long and interspersed with other smaller eskers is present at the terrestrial margin of the moraine system, adjacent to an area of glaciofluvial outwash bordering the fjord (Fig. 2D). At Skobreen there are a small number of CSRs in the forefield in an area of streamlined till. A large meltwater channel exits from a subglacial conduit in the frontal margin and cuts through the till surface adjacent to the lateral moraine ridges.

The landform record highlights the rich surge history of the

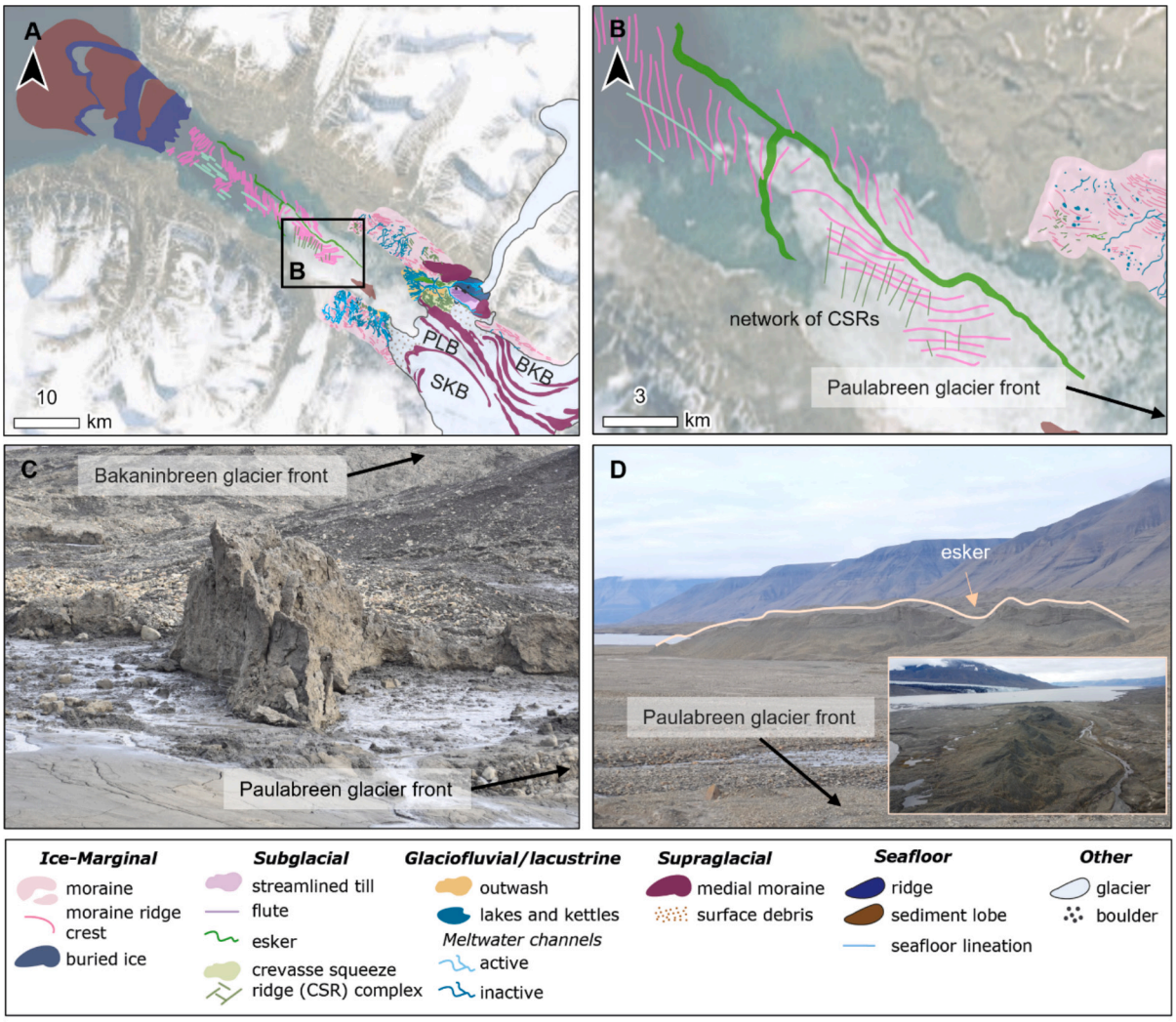

Fig. 2. Examples of key landforms in the Bakaninbreen-Paulabreen glacier system. (A) Geomorphology of the innermost terrestrial fjord margins and as mapped by Ottesen et al. (2008) on the floor of Rindersbukta. Background satellite imagery is sourced from ESRI basemap imagery. BKB = Bakaninbreen, PLB = Paulabreen, SKB = Skobreen. (B) Sinuous esker, moraine ridges and CSRs on the fjord floor as mapped by Ottesen et al. (2008). (C) Large, sharp crested CSR on the northern fjord margin photographed in 2021. View towards the south with the glacier ice front to the east. (D) Large esker at the terrestrial margin of Bakaninbreen. Inset image shows the esker on UAV imagery captured in 2021, looking towards Rindersbukta. View towards the north with glacier ice front to the east.

Bakaninbreen-Paulabreen glacier system. CSRs are ubiquitous at the ice margin on both sides of the fjord, as well as on the fjord floor (Ottesen et al., 2008). CSRs are a clear indicator of a fractured glacier base and the presence of highly saturated subglacial material, conditions characteristic of the surge active phase. Thus their presence at the margins of all three glaciers in the system, with their known surge history, and in both terrestrial and marine settings, is unsurprising. The density of kettle lakes in the distal parts of the moraine system are characteristic of in situ ice stagnation during quiescence, and contrast to the formation of retreat moraines on the fjord floor (Ottesen et al., 2008). The large esker on the north side of the fjord represents the extension of the subglacial conduit at Bakaninbreen's lateral margin that has carved a deep canyon in the moraine surface.

4.1.2. Penckbreen

The Penckbreen forefield consists of a complex network of proglacial lakes and CSRs at the ice margin. The glacier front is beginning to recede back into its large proglacial lake following the 2016–2020 surge. The forefield is enclosed by a large glaciotectonic composite ridge system cut by frequent inactive meltwater channels that marks the maximum extent of its pervious surge (Hart and Watts, 1997) (Fig. 3A), beyond which glaciofluvial outwash plains extend to the fjord. Penckbreen advanced ~2 km into its proglacial lake during the 2016–2020 surge, fragmenting the lake into series of smaller individual lakes and shunting large areas of thick lake sediment punctuated with CSRs (Fig. 3A, B, C).

Geomorphological evidence of surging is present throughout the Penckbreen forefield. The large composite ridge system represents the deformation of pre-existing forefield sediments into a glaciotectonic moraine complex during a single surge or multiple surges likely during the LIA. Such moraine systems are found at the margins of ~50 surge-type glaciers across Svalbard (e.g., Croot, 1988; Boulton et al., 1999; Schomacker and Kjær, 2008; Lovell and Boston, 2017). Inside the moraine system, the network of CSRs close to the heavily fractured glacier margin demonstrate the squeezing of deformable subglacial material into basal crevasses. The recent 2016–2020 surge advanced into the large proglacial lake and shunted large areas of lake sediments into the zone between the glacier front and the glaciotectonic composite ridge system. The proglacial lake has been fragmented by the advance into a number of isolated lakes and islands of sorted sediment to the east, with a larger lake remnant maintained to the west.

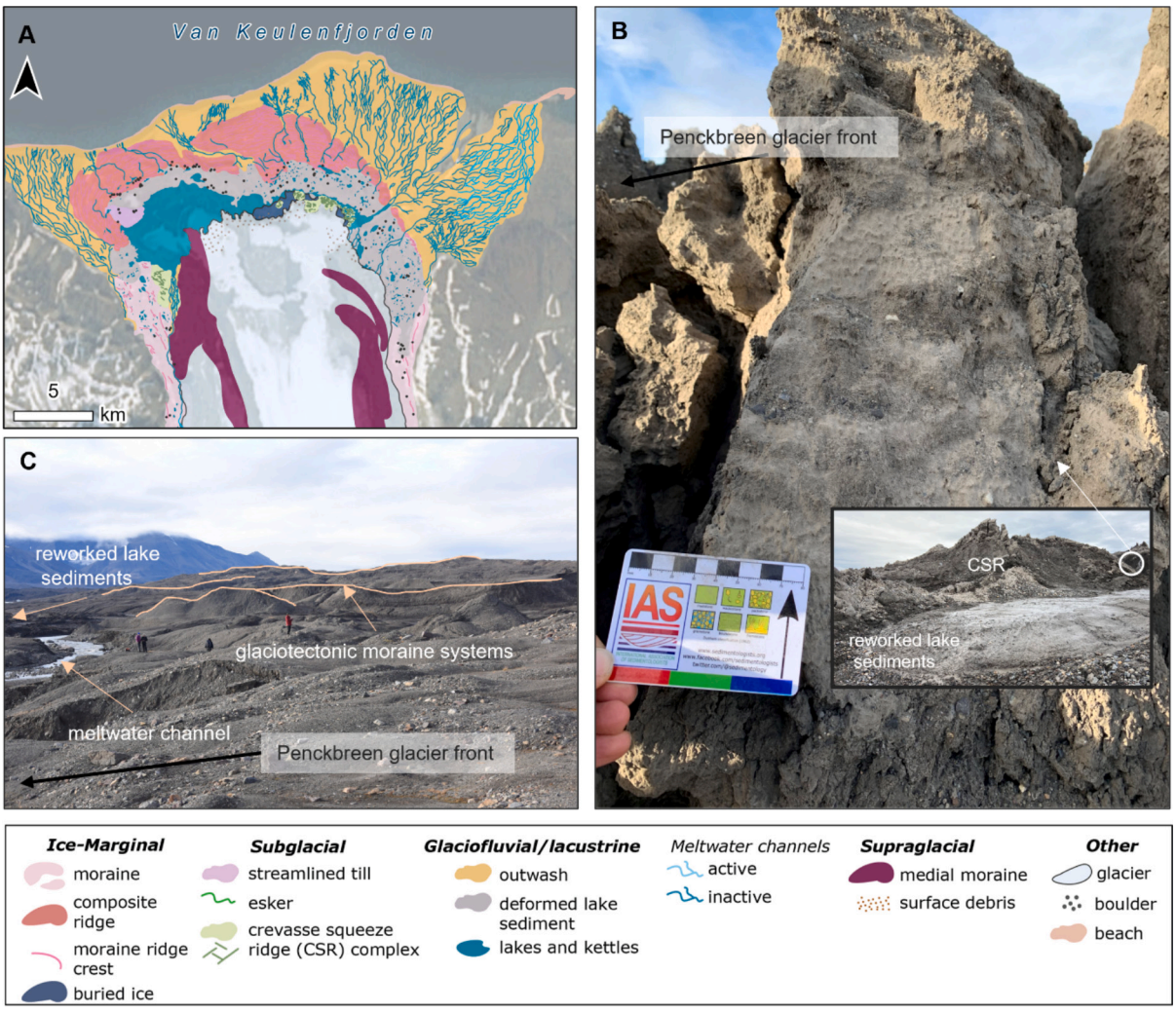

Fig. 3. Examples of key landforms at Penckbreen. (A) Geomorphological mapping of the Penckbreen forefield. Background satellite imagery is sourced from ESRI basemap imagery. (B) Internal structure of a CSR on the forefield. Inset image shows the CSR surrounded by areas of deformed lake sediments. View towards the west with glacier front to the south. (C) View across the forefield showing areas of deformed lake sediments and active meltwater channels bound by the large glaciotectonic moraine system.

4.1.3. *Antoniabreen*

An arcuate latero-frontal moraine system encloses a large glaciofluvial outwash plain that dominates the forefield (Fig. 4A, D). The active channel system breaches the moraine ridge to the northwest before draining a further ~1.5 km to the fjord. The extensive outwash plain in the inner forefield contains large areas of inactive channels, particularly to the east, where some of the relict channels are orientated parallel to the glacier margin (Fig. 4C, D). The lateral part of the moraine system may have experienced some slope instabilities and reworking evidenced by their slumped and deflated morphology (Fig. 4B). Aside from the outwash, there are small patches of streamlined tills to the west and kames to the east (Fig. 4B). Aerial photographs viewed on the Norwegian Polar Institute (NPI) *TopoSvalbard* online archive (toposvalbard.npolar.no) from 2011 and ESRI Basemap imagery show areas of proglacial icing centred around the main active meltwater drainage.

The lateral-frontal moraine system is likely ice-cored based on the observed areas of re-working, indicating degradation of buried ice bodies as described in Schomacker and Kjær (2008) and Ewertowski and Tomczyk (2020) studies in Svalbard. The patches of kame and kettle topography also suggest the presence of buried ice. The inner forefield is dominated by outwash, with some isolated areas of streamlined till. In the eastern part of the outwash, relict channels oriented perpendicular to the ice margin suggest meltwater has been routed along the frozen margin. Together, these key features are indicative of current polythermal glacier conditions as suggested for other Svalbard glaciers by Glasser and Hambrey (2005).

4.1.4. *Renardbreen*

The glacier forefield of Renardbreen is bound by a well-defined latero-frontal moraine system (Fig. 5A). The eastern section of the moraine ridge complex is not complete and presumably extends into Josephbukta, indicating that the glacier has previously been partially marine-terminating. The forefield is dominated by glaciofluvial outwash (Fig. 5B) with frequent inactive meltwater channels that run parallel to the glacier front, and areas of proglacial icing adjacent to the active channel. The outwash is punctuated by patches of streamlined till surfaces (Fig. 5C) with small flutes that typically have boulders at the head (Fig. 5D). The current active drainage corridor emerges from the centre of the glacier and drains eastwards to the fjord. A series of small eskers and lakes are found close to the active channels. In the southern section of the forefield, just inside the bounding latero-frontal moraine system, small areas of CSRs are found on streamlined till surfaces (Fig. 5A).

The Renardbreen forefield is strongly indicative of current polythermal conditions with evidence for past dynamic flow. The meltwater dominance in the forefield, coupled with areas of well-developed

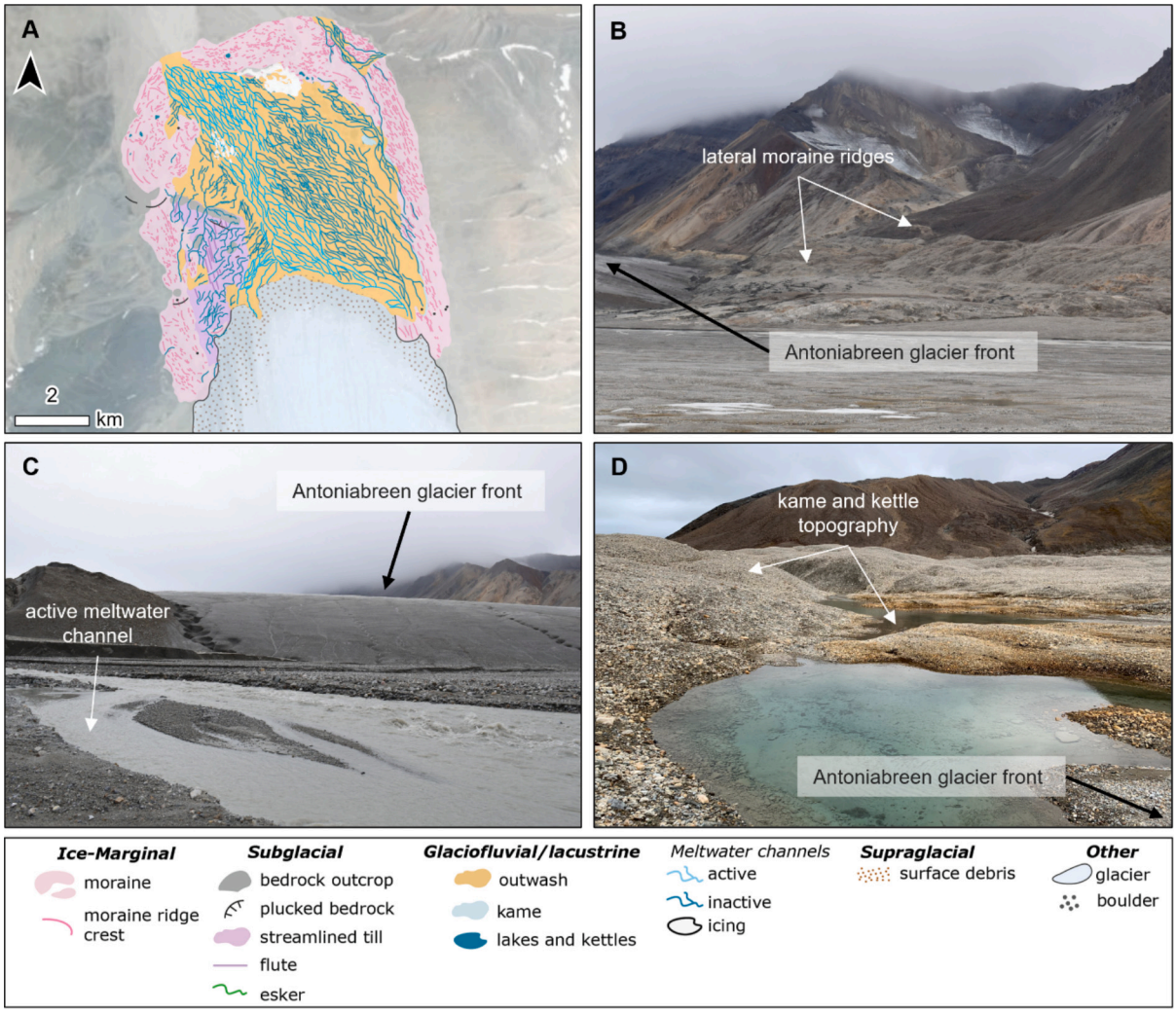

Fig. 4. Examples of key landforms at Antoniabreen. (A) Geomorphological map of the Antoniabreen forefield. Background satellite imagery is sourced from ESRI basemap imagery. (B) Lateral moraine ridges and the extensive glaciofluvial outwash plain. View towards the west. (C) Active meltwater channel emanating from the glacier front. View towards the south and glacier front. (D) Kame and kettle topography on the eastern edge of the glacier forefield. View towards the east with the glacier front to the south.

flutings demonstrates warm-based flow. The series of relict meltwater channels aligned perpendicular to the ice margin suggest drainage guided by a frozen and impermeable glacier front as stated in Aradóttir et al. (2019) and Hättestrand and Stroeven (2002), tracking a steadily retreating margin over time. The presence of small areas of CSRs in the southeast part of the forefield, together with the patches of streamlined till, suggests past dynamic flow characteristic of surging. Although Renardbreen has not been directly observed to surge, it is possible this past inferred dynamism occurred when the glacier was marine-terminating, as evidence by the latero-frontal moraine potentially extending into the fjord, prior to the early 1990s as suggested by Zagórski et al. (2023).

4.1.5. Scottbreen

The Scottbreen forefield is enclosed by a latero-frontal moraine system that is particularly well-developed on the southeast side (Fig. 6A). The inner forefield contains large areas of streamlined till and flutes (in central areas; Fig. 6C) and supraglacial sediment drapes with proglacial striping and bedrock exposures (close to the thin ice margin), and in general is far less dominated by outwash than Antoniabreen and Renardbreen. The active drainage forms a narrow breach through the frontal moraine system before draining ~1.5 km to the mouth of Recherchefjorden. The glaciofluvial outwash within the inner forefield contains a mixture of active and inactive meltwater channels (Fig. 6B, C), all of which converge towards the narrow breach in the moraine. An area of proglacial icing is visible close to the moraine breach on both aerial imagery viewed on the NPI *TopoSvalbard* online archive (toposvalbard.npolar.no) from 2011 and ESRI Basemap imagery. A small area of kame topography is present close to the southern ice margin and an area of buried ice (Fig. 6A).

The dominance of supraglacial landforms such as supraglacial sediment drapes and debris stripes close to a thin ice margin suggest that parts of Scottbreen may be largely cold-based, particularly in the northwest part of the glacier front. This landform assemblage is also typical in the Alpine vanishing glacier landsystem based on Pasterze Glacier, Austria (Le Heron et al., 2022). This interpretation is further supported by the more spatially-restricted glaciofluvial activity evidence in the forefield, which is largely focused immediately around the current main meltwater channel. However, the extensive areas of flutes and streamlined till surfaces demonstrate warm-based conditions are also recorded in the forefield, potentially associated with one or more periods of past ice expansion coinciding with the formation of the moraine complex.

4.1.6. Bullbreen

The Bullbreen forefield extends to St. Jonsfjorden and is bound by

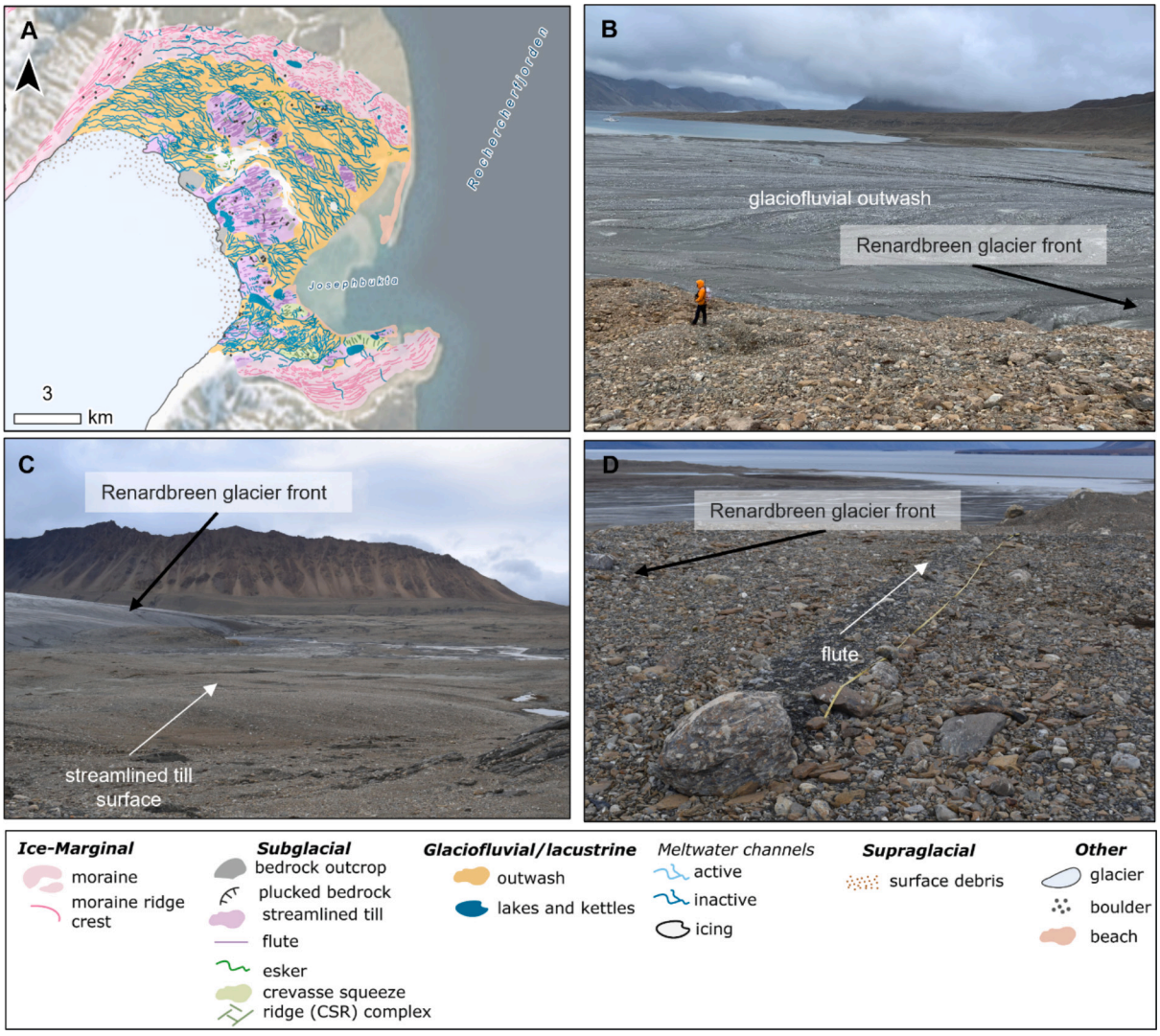

Fig. 5. Examples of key landforms at Renardbreen. (A) Geomorphological map of the Renardbreen forefield. Background satellite imagery is sourced from ESRI basemap imagery. (B) Well-developed glaciofluvial outwash plain extending to Josephbukta in the distance. View towards the east with glacier front to the west. (C) Streamlined till surface close to the southern glacier margin. View towards the north. (D) A flute with a boulder at its head, with Recherchefjorden visible in the background. View towards the east.

large lateral moraines (Fig. 7A). Inside the moraines, the central forefield contains areas of outwash and streamlined till surfaces, with the latter particularly well-preserved in eastern areas, including one section that extends to the fjord, and close to the ice margin on both sides. Flutes are also emerging from the glacier snout (Fig. 7D). At the western ice margin, flutes are interspersed with supraglacial debris stripes and boulder trains, where boulder trains are composed of larger boulder-sized material, both on the ice surface and emerging into the proglacial forefield (Fig. 7B, C, D). Within the areas of outwash, inactive channels closest to the ice margin in the eastern part of the forefield are orientated parallel to the glacier front, and in central areas drain directly towards the fjord (Fig. 7A). NPI *TopoSvalbard* online archive (toposvalbard.npolar.no) from 2011 and ESRI Basemap imagery demonstrates that proglacial icings form within the central areas of active meltwater drainage.

The extension of the lateral moraines and central area of flutings to the fjord shore, with no frontal moraine system apparent in a terrestrial position, indicates that Bullbreen extended into the fjord at its most-recent maximum position – likely similar to other currently land-terminating glaciers in the inner part of St. Jonsfjorden (e.g. Farnsworth et al., 2017). The fluted zones and large active outwash plain (plus proglacial icing) are indicative of polythermal conditions, with a frozen margin suggested by the ice front-parallel relict channels in the east of the forefield (Fig. 7A) and supraglacial debris stripes and boulder trains at the western margin (e.g., Le Heron et al., 2022) (Fig. 7B).

4.1.7. *Charlesbreen*

The Charlesbreen forefield is bound by well-established lateral moraine areas that extend to St. Jonsfjorden (Fig. 8A). Close to the ice margin, there is clear evidence that the moraine area is ice-cored (Fig. 8b). The central forefield is dominated by a large lagoon connected to the fjord in a distal position, and by an extensive outwash plain immediately in front of the glacier margin. A large proglacial icing is visible on the outwash plain in imagery sourced from the NPI *TopoSvalbard* online archive (toposvalbard.npolar.no) from 2011 and ESRI Basemap images. At the southern ice margin, an area of streamlined till extends discontinuously to the fjord, with isolated pockets of streamlined till also found within the large areas of outwash. A large complex of kame and kettle topography cut by inactive meltwater channels aligned perpendicular to the ice margin is found close to the northern lateral moraine and the glacier front (Fig. 8C, D).

Similar to Bullbreen, the extension of the moraine systems to the

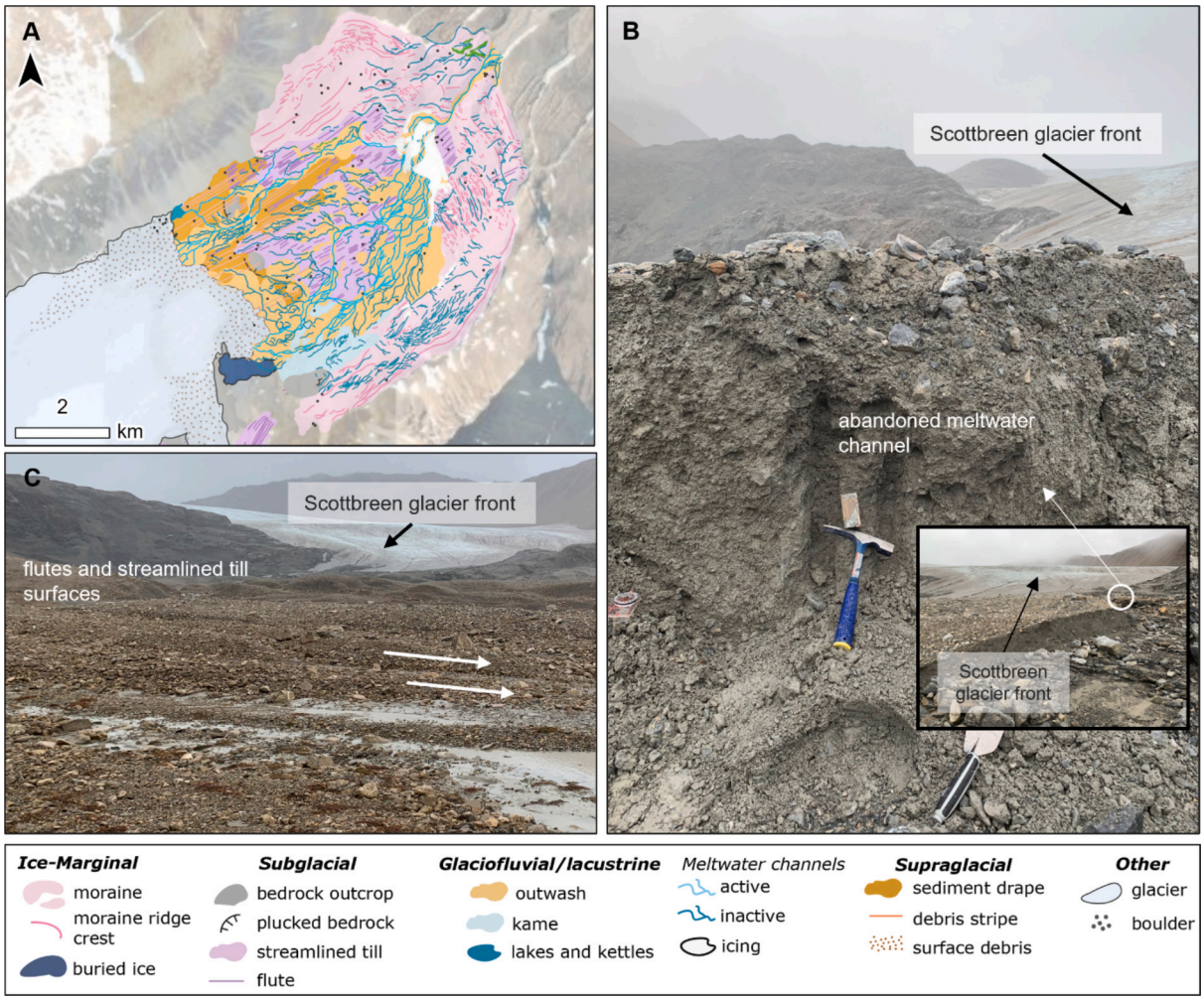

Fig. 6. Examples of key landforms at Scottbreen. (A) Geomorphological map of the Scottbreen forefield. Background satellite imagery is sourced from ESRI basemap imagery. (B) Internal composition of an abandoned meltwater channel. View towards the southwest. Inset image shows the abandoned meltwater channel surrounded by glaciofluvial outwash. (C) Flutes and streamlined till surface on the forefield. View towards the northwest.

fjord shows that the glacier terminated in a marine setting at its most-recent maximum positions, and indeed there is a corresponding arcuate ridge mapped at this location using bathymetry data in Farnsworth et al. (2017). There is clear evidence that the lateral moraine systems are ice-cored. Overall the extensive outwash plain dominating the forefield, coupled with areas of fluted and streamlined till surface, are characteristic of polythermal conditions, which may be further supported by the presence of an extensive proglacial icing.

4.1.8. Protektorbreen

The Protektorbreen forefield extends to Trygghamna and is dominated by exposed bedrock, thin streamlined till surfaces and supraglacial debris stripes, with small patches of glaciofluvial outwash and inactive meltwater channels (Fig. 9A). Towards the north of the forefield the inactive channels trace the former ice margin. Small, isolated areas of proglacial icing are visible along the main active channel on NPI *TopoSvalbard* online archive (toposvalbard.npolar.no) imagery from 2011 and ESRI Basemap imagery. The ice margin is thin (Fig. 9B), <10's m of ice thickness and supraglacial debris stripes can be traced into the forefield (Fig. 9C). A small lateral moraine ridge approximately 2 km long borders the southern edge of the forefield.

The limited evidence of glaciofluvial processes and subglacial landforms combined with the dominance of exposed bedrock and only thin debris cover with extensive supraglacial debris stripes suggests Protektorbreen is largely experiencing cold-based conditions. Inactive meltwater channels tracing the ice front suggest meltwater routing along a retreating frozen margin. There is limited active meltwater activity within a restricted outwash area, with occasional small patches of proglacial icing. Whilst icings have been associated with polythermal conditions (e.g., Hagen et al., 2003), they are also found in front of many glaciers assumed to be largely cold-based (e.g., Mallinson et al., 2019). In its current configuration, Protektorbreen has disconnected from a larger accumulation area, meaning it is now a completely isolated ice mass at the valley head. However, it has clearly been part of a much larger contiguous glacier system that extended into Trygghamna, outlined in Aradóttir et al. (2019), at its most-recent maximum extent.

4.1.9. Ferdinandbreen

The Ferdinandbreen forefield is dominated by steep lateral moraines extending downvalley to a frontal position ~2 km from the current ice margin (Fig. 10A). The central part of the forefield is narrow and primarily covered by glaciofluvial outwash and thin supraglacial sediment drapes. Supraglacial debris stripes can be traced from the glacier surface into the forefield, where they can extend for hundreds of metres (Fig. 10A, B). The glacier snout is heavily fragmented by large bedrock outcrops (Fig. 10C) and since 2021 has become completely disconnected from its larger accumulation areas.

There is limited evidence of active glacial processes occurring at Ferdinandbreen with no active meltwater channels, depositional features or erosional indicators. The moraine system tracks the previous

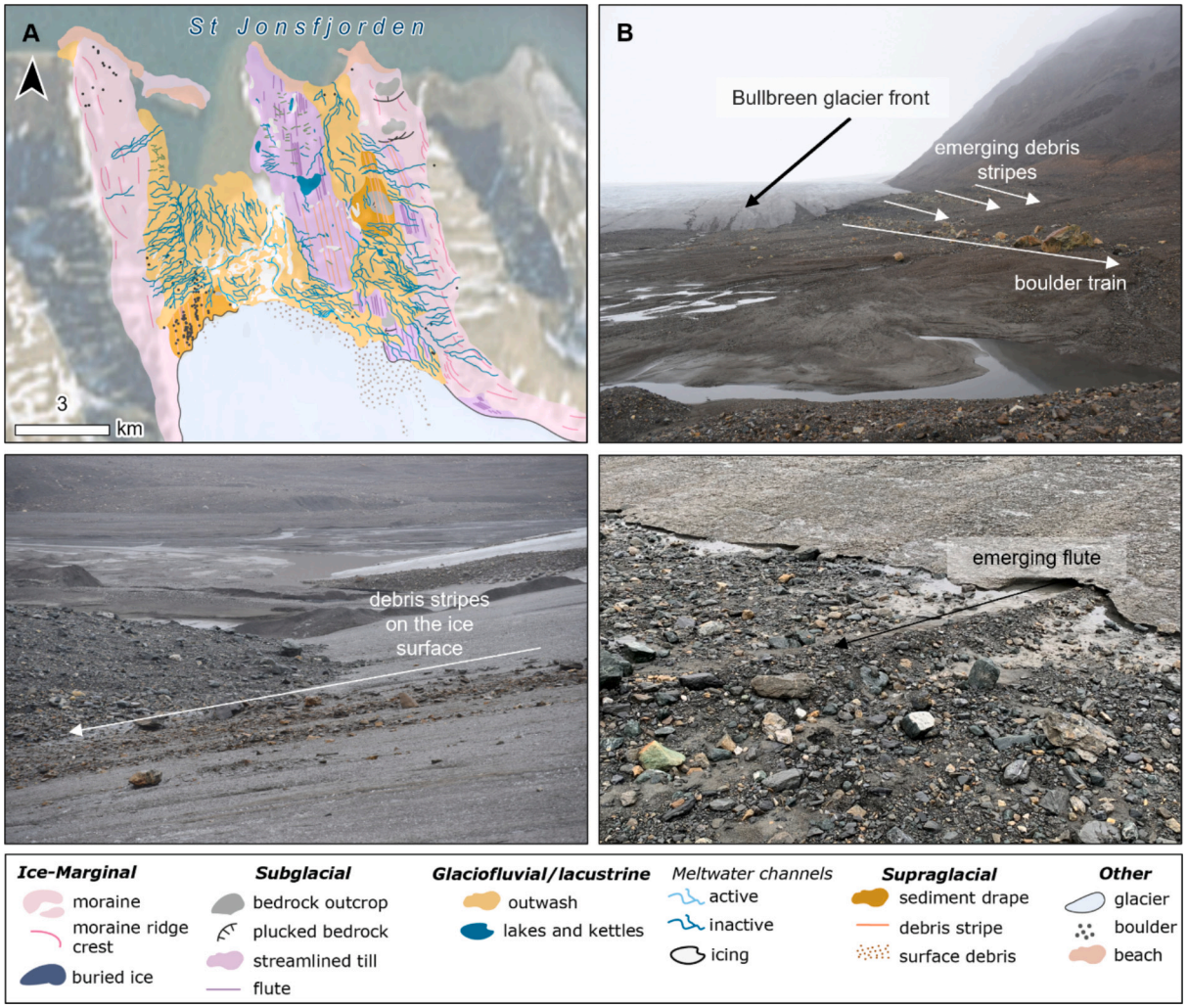

Fig. 7. Examples of key landforms at Bullbreen. (A) Geomorphological map of the Bullbreen forefield. Background satellite imagery sourced from ESRI basemap imagery. (B) The western part of the forefield with supraglacial debris stripes and boulder trains. View towards the south and the glacier front. (C) Bullbreen ice surface with supraglacial debris stripes. View towards the east across the glacier snout. (D) A flute emerging from beneath the Bullbreen glacier snout. View towards the east.

extent of the glacier which flowed downvalley and at some point, had an active meltwater system as evidenced by the abandoned meltwater channels and eskers at the end of the valley. The dominance of thin sediment cover and debris stripes in the forefield close to the current ice margin suggests extensive ice freeze-on to the bed at minimum at the glacier margins, however owing to the small glacier size, likely across the whole of the glacier. The predominant deposition at this glacier is by meltout due to glacier recession as opposed to active subglacial deposition from warm-based or polythermal regimes. The emergence of large bedrock outcrops resulting in the fragmentation of glacier ice may be enhancing thinning and freeze-on of ice by driving separation of the glacier tongue with a higher elevation accumulation area. Ferdinandbreen is therefore interpreted to be a vanishing glacier.

4.2. Glacier landsystem models

Here, we synthesize the geomorphological evidence presented for the 11 glaciers into four landsystem models, with additional support from previous studies that fit into the different landsystem categories. We present landsystems for (1) marine-terminating surge-type glaciers; (2) land-terminating surge-type glaciers; (3) polythermal valley glaciers; and (4) small vanishing glaciers.

4.2.1. Marine-terminating surge-type glacier landsystem

The marine-terminating surge-type glacier landsystem (Fig. 11) contains both seafloor and terrestrial components and is based on our observations and the Ottesen et al. (2008) mapping from the Bakaninbreen-Paulabreen glacier system (Fig. 2A, Table 2). This is further supported by additional insights into the submarine and terrestrial geomorphological records of marine-terminating surge-type glaciers provided by several studies (e.g. Boulton et al., 1996; Ottesen and Dowdeswell, 2006; Ottesen et al., 2008, Ottesen et al., 2017; Flink et al., 2015; Lovell et al., 2018b; Aradóttir et al., 2019; Osika and Jania, 2024).

Several key landforms are found on both the seafloor and at the terrestrial fjord margins that can be linked to processes during the surge cycle. The maximum extent of surge advances is typically marked by a large glaciotectonic ridge on the seafloor with suites of small transverse retreat moraines formed during quiescent-phase recession within those limits (Ottesen et al., 2008; Flink et al., 2015; Ottesen et al., 2017; Aradóttir et al., 2019). The retreat moraines are formed by minor winter readvances (e.g. Flink et al., 2015), and contrast to the widespread in situ ice stagnation that takes place at the terrestrial margin. Low-angle debris flow lobes are a common feature that extend from the distal flank of submarine glaciotectonic moraines, reflecting rapid sedimentation of soft subglacial tills during the surge (Ottesen and Dowdeswell, 2006; Ottesen et al., 2008; Ottesen et al., 2017; Aradóttir et al., 2019).

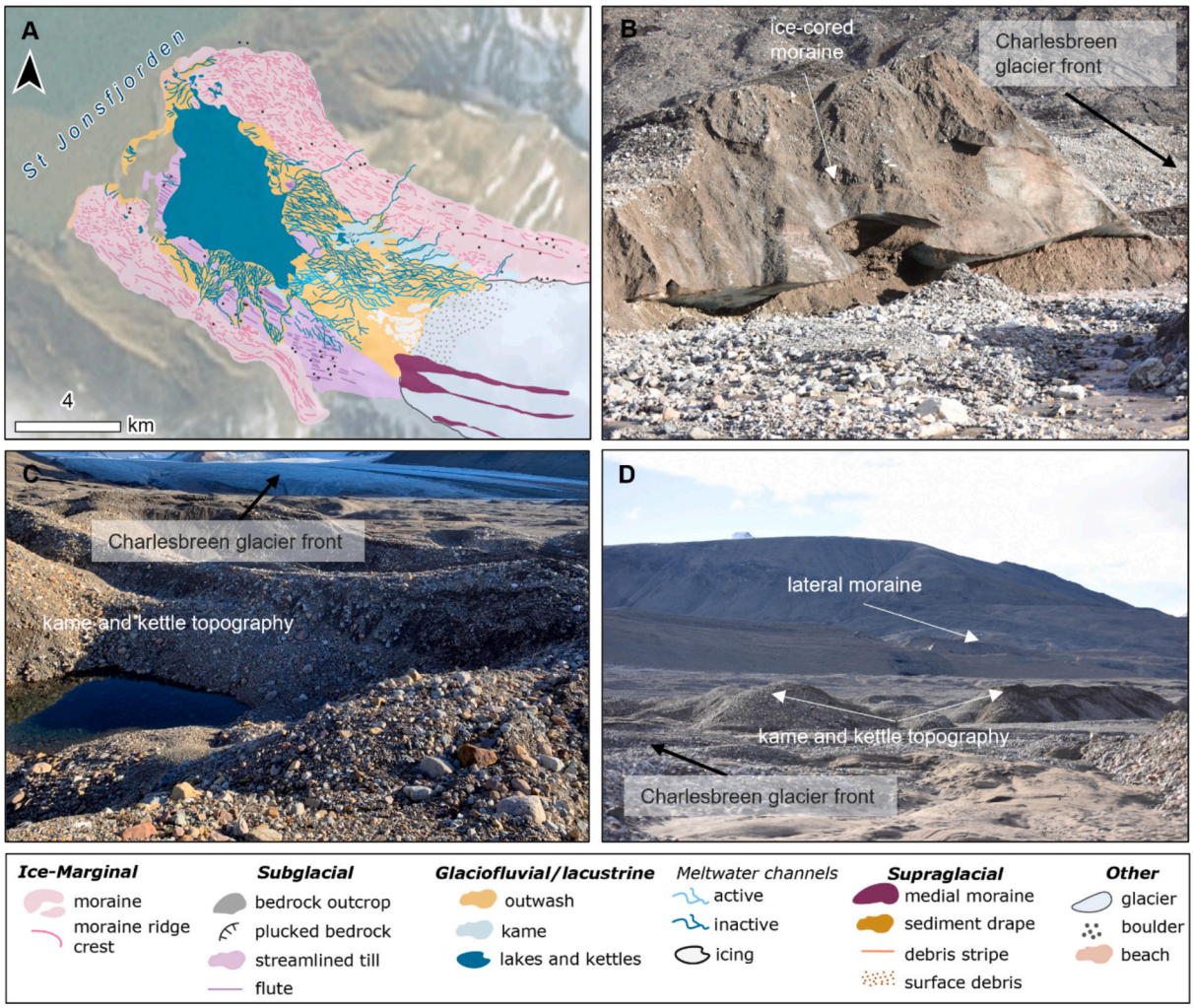

Fig. 8. Examples of key landforms at Charlesbreen. (A) Geomorphological map of the forefield. Background satellite imagery sourced from ESRI basemap imagery. (B) Section through ice cored moraine. View towards the east with the glacier front to the south. (C) Kame and kettle topography close to the northern ice margin. View towards the southwest and glacier front. (D) View southeast across the forefield towards the southern lateral moraines, with the kame and kettle topography at the northern ice margin visible in the foreground.

The inclusion of a terrestrial component to the marine-terminating surge-type glacier landsystem captures the geomorphological activity at the fjord margins during marine-terminating surges. At the terrestrial fjord margins, it is common for the lateral splaying of ice to form similar glaciotectonic moraine systems in a terrestrial position, sometimes through the onshore movement of marine muds (e.g. Kristensen et al., 2009; Lovell et al., 2018b). CSRs are usually ubiquitous on both the seafloor and at the terrestrial margins. During a surge, both the glacier surface and the bed become heavily crevassed due to the increase in ice flow velocities (Sharp, 1985; Evans and Rea, 1999; Woodward et al., 2002, 2003). Saturated subglacial sediment is squeezed up into the fractured glacier base as the ice begins to stagnate towards the end of the surge, creating cross-cutting ridges that mimic crevasse orientations (Sharp, 1985; Evans and Rea, 1999; Woodward et al., 2003). CSRs were identified at all surge-type glacier forefields analysed here and is typically reflected in surge-type glacier landsystem models for Svalbard (e.g. Evans and Rea, 1999; Ottesen et al., 2008), barring the Aradóttir et al. (2019) model.

Flutings and glacial lineations are also found both on the seafloor and at the fjord margins but tend to be far longer and better preserved in a submarine setting. Eskers are also common in both settings, with seafloor eskers often found to extend from the location of subglacial portals (e.g. Ottesen and Dowdeswell, 2006). Similar to flutes/glacial lineations, eskers tend to be longer and better preserved on the seafloor. These landforms extending in the submarine zone expands on the previously published models by Aradóttir et al. (2019) which does not present these landforms in their model of the marine and terrestrial margins of surging glaciers.

The main difference between the seafloor and terrestrial records is the presence of retreat moraines formed during quiescent-phase recession on the seafloor (e.g. Flink et al., 2015). These are not found at the terrestrial fjord margins, where the quiescent phase is characterised by in situ subaerial ice stagnation and downwasting, forming hummocky terrain (kame and kettle topography), large volumes of buried ice and active debris flows (see, Schomacker and Kjær, 2008). Meltwater outwash also typically dominates the terrestrial margins, often forming deltas where the stream enters the fjord.

4.2.2. *Land-terminating surge-type glacier landsystem*

The land-terminating surge-type glacier landsystem is based on our observations from Penckbreen, supported by previous work on land-terminating surges in Svalbard (e.g. Hart and Watts, 1997; Boulton et al., 1999; Ottesen et al., 2008; Lønne, 2016; Lovell et al., 2018a; Aradóttir et al., 2019). Key landforms include CSRs, flutes, eskers and, in some cases, large glaciotectonic moraine systems and proglacial lakes (see Lovell and Boston, 2017) (Fig. 3; Fig. 12; Table 2).

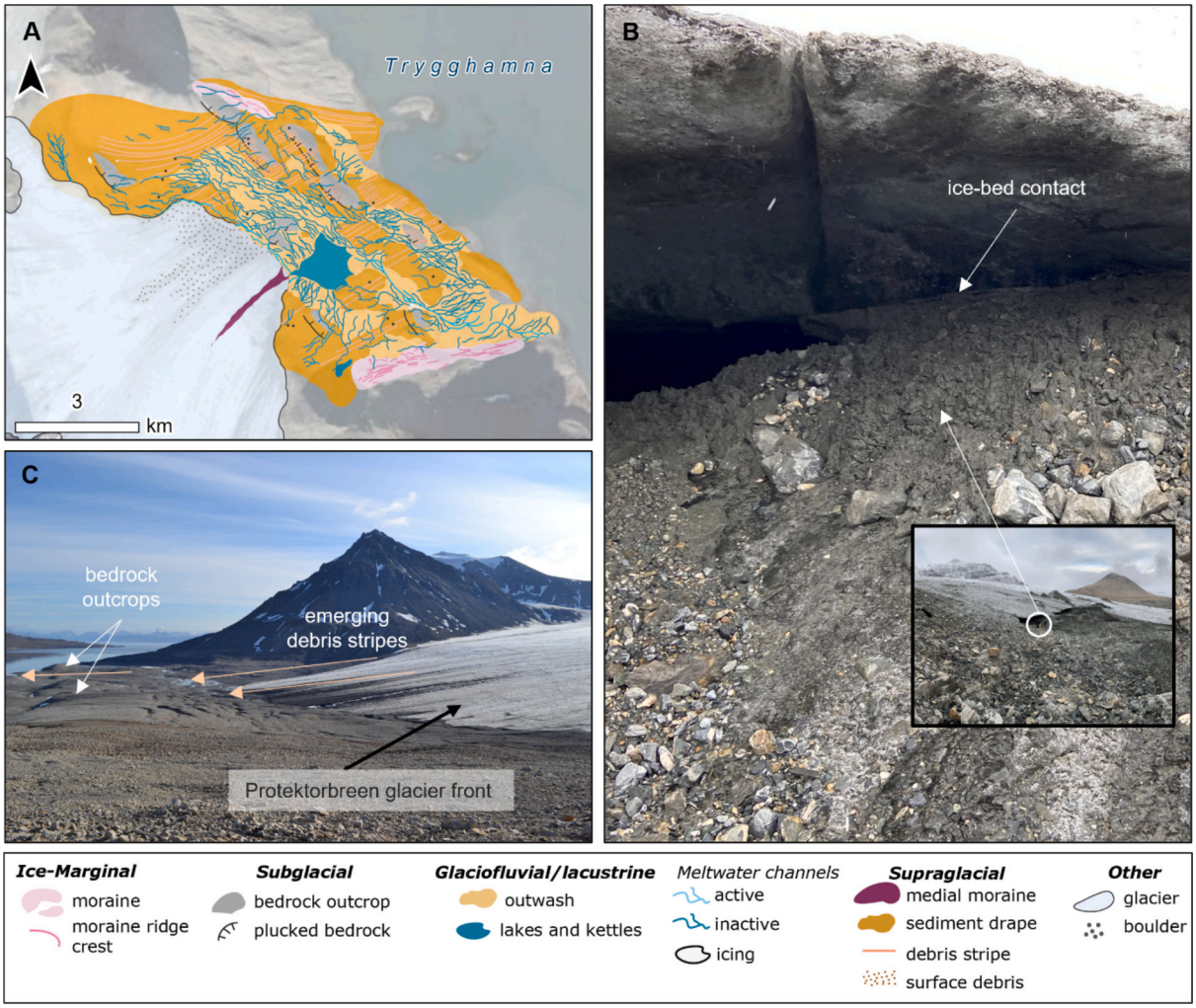

Fig. 9. Examples of key features at Protektorbreen. (A) Geomorphological map of the forefield. Background satellite imagery sourced from ESRI basemap imagery. (B) Ice-bed contact of the thin glacier front. View towards the north at the lateral ice margin. (C) Supraglacial debris stripes extending out into the forefield. Note the exposed bedrock in several places. View towards the south.

The most characteristic landform type in land-terminating surge-type glacier landsystems is arguably CSRs (e.g. Sharp, 1985; Rea and Evans, 2011; Farnsworth et al., 2016; Ingólfsson et al., 2016; Aradóttir et al., 2019; Ben-Yehoshua et al., 2023). Flutes (e.g. Christoffersen et al., 2005) and zig-zag eskers, formed by meltwater occupation of the basal crevasse system (e.g. Evans et al., 2022), have also been reported. Penckbreen has a large glaciotectonic moraine system. Such moraine systems are found at several surge-type glaciers in Svalbard, sometimes also in combination with lakes (Boulton et al., 1999; Schomacker and Kjær, 2008; Lovell and Boston, 2017). Glaciotectonic moraine systems can be formed in single surge events (e.g. Hagen, 1988; Hart and Watts, 1997) or through the piggy-backing of multiple ridges formed during a series of surges to similar positions (Lovell et al., 2018a). Whilst there is a strong correlation between the presence of glaciotectonic moraine systems and surge-type glaciers (e.g. Croot, 1988; Lovell and Boston, 2017), they are certainly not ubiquitous at land-terminating surge-type glaciers in Svalbard. Widespread evidence for subaerial ice stagnation and downwasting in the form of kame and kettle topography and debris flows is also common, representing quiescent phase recession.

Our land-terminating surge-type glacier landsystem model shares similarities with a previous surge landsystem models presented for Svalbard. For example, Aradóttir et al. (2019) modelled terrestrial surge margins and also highlighted the presence of flutes, CSRs and hummocky moraine deposits. However, they also highlighted supraglacial and englacial debris deposits in the forefield, whereas Penckbreen was dominated by proglacial (e.g. glaciotectonic pushing of lake sediments) or subglacial (e.g. CSR) features.

There are also similarities between our landsystem models and those based largely on Icelandic examples (e.g. Evans and Rea, 1999; Evans et al., 2009; Schomacker et al., 2014; Ingólfsson et al., 2016). Key features present in these examples include glaciotectonic moraine systems, CSRs, flutes and eskers. In comparison to Icelandic land-terminating surge landsystem models, the well-developed and often extensive channelled outwash plains with pitted deposits and kettle holes (e.g. Russell et al., 2001; Björnsson et al., 2003; Evans et al., 2009; Schomacker et al., 2014) are less well developed in the Svalbard landsystem.

4.2.3. *Polythermal valley glacier landsystem*

The polythermal valley glacier landsystem is based on Antoniabreen, Renardbreen, Scottbreen, Bullbreen and Charlesbreen (Fig. 13, Table 2). This suite of polythermal glaciers includes independent glaciers (Renardbreen, Scottbreen, Bullbreen) and those connected to larger icefields (Antoniabreen, Charlesbreen). These examples of polythermal valley glaciers mostly fall within the bottom-heavy hypsometric range (Table 1), meaning most of their mass is located at lower elevations and thus more susceptible to temperature perturbations (Noël et al., 2020).

The landsystem is characterised by ice-cored latero-frontal moraine complexes, although where the glaciers have extended into fjords at

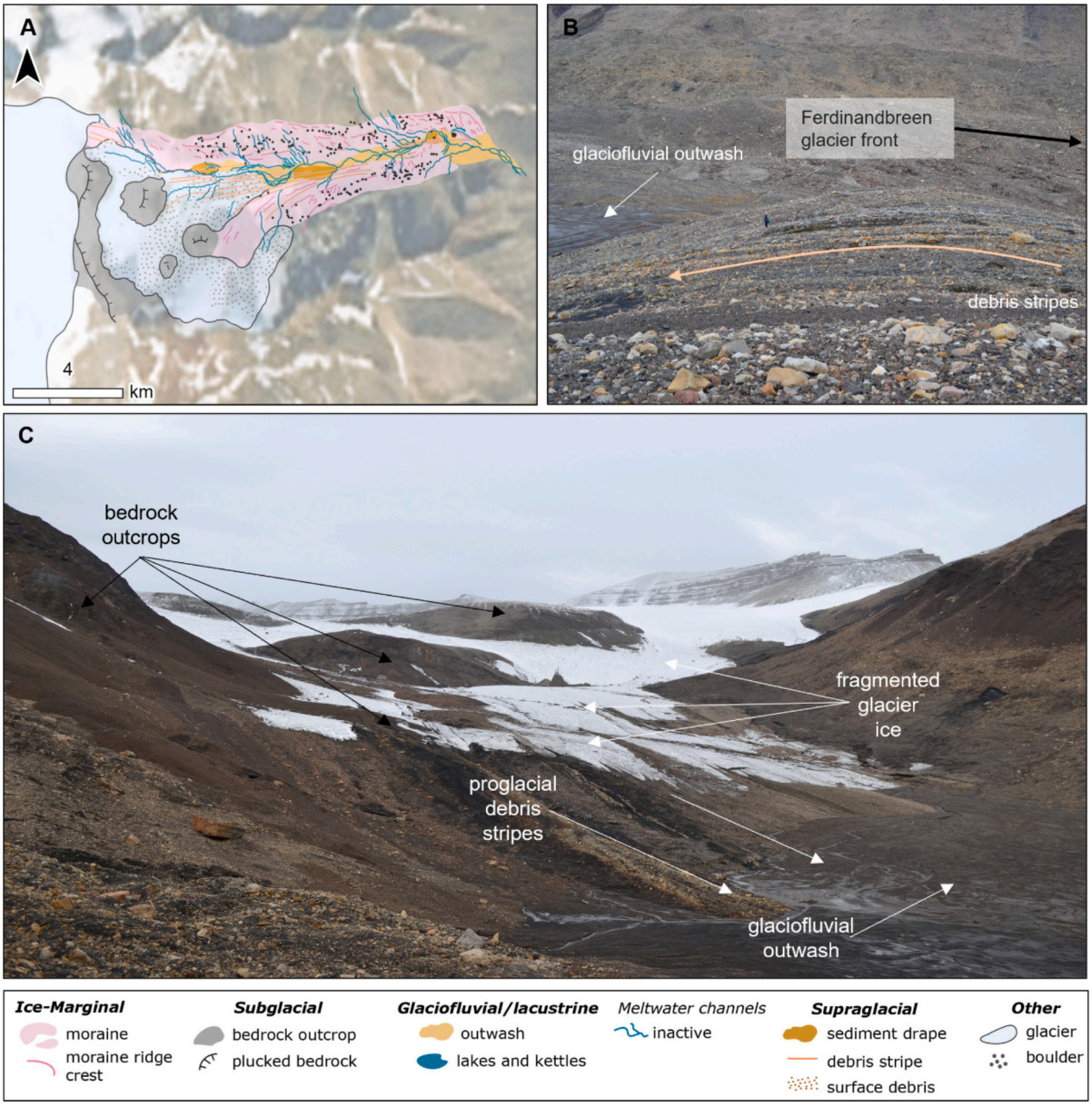

Fig. 10. Examples of key features at Ferdinandbreen. (A) Geomorphological map of the Ferdinandbreen forefield. Background satellite imagery sourced from ESRI basemap. (B) Supraglacial debris stripes in an area of thin supraglacial sediment drape, with the southern steep lateral moraine in the background. View towards the south with the ice front to the west. (C) View west towards the glacier in 2016, highlighting the fragmentation of the thinning glacier ice around emerging bedrock outcrops. Ferdinandbreen has since disconnected from the larger source areas visible in the top right of the image. Supraglacial debris stripes are visible extending into the forefield.

their most-recent maximum position, the frontal parts of the moraine system may be missing on land (e.g. Renardbreen, Bullbreen, Charlesbreen). Inside the moraine systems, the forefields are dominated by extensive active and inactive outwash plains, evidencing spatially dynamic hydrological systems. Inactive outwash plains often contain suites of relict channels oriented parallel to the ice front, suggesting meltwater tracing of a frozen, impermeable ice margin during recession. Proglacial icings are common at all glaciers within this category and have previously been suggested to be indicative of polythermal conditions (Hagen et al., 2003), although it is important to note that icings are also found at presumed cold-based glaciers (Mallinson et al., 2019).

Flutes and streamlined till surfaces are abundant at all the glaciers falling within this category and are a good indicator of an active subglacial environment in a temperate or polythermal regime. Such streamlined subglacial landforms have been observed to have formed at polythermal Svalbard glaciers where fine saturated sediment is squeezed into a basal cavity that forms on the lee side of large boulders or obstacles (e.g. Glasser and Hambrey, 2005; Ottesen and Dowdeswell, 2006; Roberson et al., 2011; Evans et al., 2022).

Buried ice is found throughout the forefields, particularly in laterofrontal moraine systems, and the subsequent melting of ice bodies develops into kame and kettle topography and hummocky moraine (Glasser and Hambrey, 2005). Such terrain found in close association with well-developed subglacial bedforms is a key indicator of polythermal conditions in recently deglaciated landscapes (e.g. Evans, 2009; Evans et al., 2012; Tonkin et al., 2016; Ewertowski and Tomczyk, 2020), and is included in the polythermal glacier landsystem model in Glasser and Hambrey (2005) as 'moraine mound complexes' in the unconfined proglacial zone.

The landsystem we propose here is comparable to that of the more

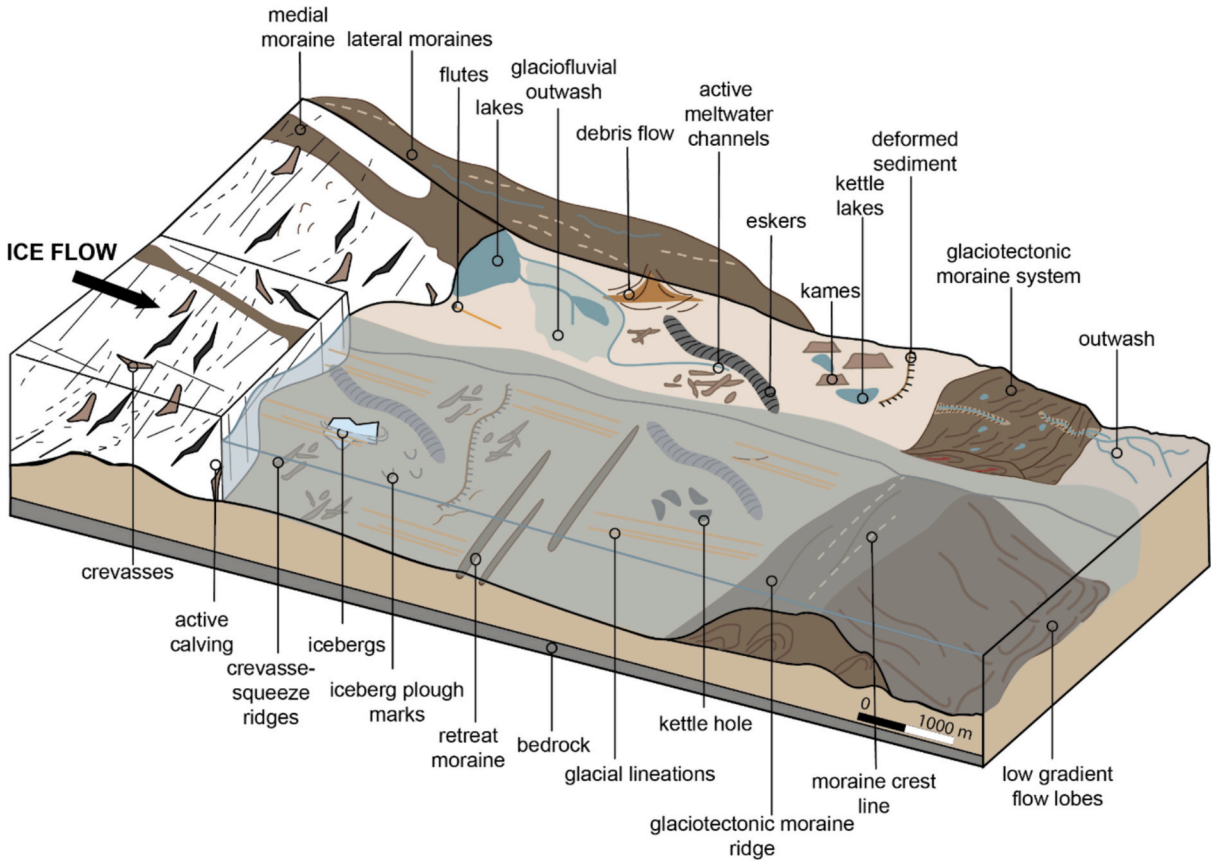

Fig. 11. Marine-terminating surge-type glacier landsystem, showing both the seafloor and terrestrial components.

simplified Glasser and Hambrey (2005) polythermal glacier landsystem, characterised by an encapsulating ice-cored outer moraine ridge with an inner moraine mound complex (hummocky moraine/ice stagnation terrain) and zone of streamlined till surfaces and flutes. One main difference we find is the dominance of glaciofluvial outwash within the inner zone: Glasser and Hambrey (2005) largely show extensive outwash limited to areas beyond the frontal moraine ridge, whereas we find it to be ubiquitous within all inner forefields.

4.2.4. *Small vanishing glacier landsystem*

The small vanishing glacial landsystem (Fig. 14) encapsulates glaciers that are likely to be almost entirely cold-based with negligible ice flow and limited meltwater activity at the terminus. In the case of Protektorbreen and Ferdinandbreen, they have effectively lost connection to a larger accumulation area, making them completely isolated ice masses. Analysis of the glacier properties shows that the vanishing glaciers are the smallest (2–4 km in length, 1–7 km^2 in area) of all the glaciers investigated here. These glaciers have either bottom heavy or very bottom-heavy hypsometric indices (Table 1), potentially exacerbating their vulnerability to future complete mass loss.

Common characteristics of the forefields consist of thin sediment drapes with frequently exposed bedrock. Forefields are dominated by supraglacial landforms, such as supraglacial debris stripes. This is also seen in the Alpine vanishing glacier landsystem based on Pasterze Glacier, Austria (Le Heron et al., 2022). Further downvalley, relict meltwater channels and glaciofluvial outwash plains are bound by well-defined lateral and terminal moraines, including LIA moraines marking past glacial extent and glacier surface height. Active meltwater drainage is minimal and spatially constrained, with some evidence for small proglacial icings (e.g. at Protektorbreen). The glaciers themselves are not only disconnected from larger source areas, but in the most extreme cases are also becoming very thin and heavily fragmented, as is the case of Ferdinandbreen (Fig. 10C).

5. Discussion

5.1. *Landsystem evidence for transitions in glacier dynamics*

Whilst many of the glaciers that fit within the polythermal landsystem category are currently thinning and relatively inactive, there is often evidence for past dynamism. This suggests that the polythermal landsystem represents an intermediate step between past dynamism, likely during the LIA or early part of the 20th century, and future thinning and fragmentation as represented by the small vanishing glacier landsystem. For example, there are several areas of CSRs at Renardbreen (Farnsworth et al., 2017; McCerery et al., 2024), which, coupled with the extensive areas of streamlined till and flutings, indicate a much more dynamic past when the glacier partly terminated in the fjord (e.g. Zagórski et al., 2023). Equally, Bullbreen and Charlesbreen have both also been much more-extensive and terminated in the fjord at their most recent maximum position, presumed to be during the LIA (e.g. Martín-Moreno et al., 2017). There are other examples of glaciers in Svalbard that would currently fit in the polythermal, or even vanishing, glacier landsystems, but were far more dynamic during the LIA (e.g. Lovell et al., 2015; Mannerfelt et al., 2024b). However, it is important to note that these glaciers rarely preserve geomorphological evidence for this past dynamism.

Under continued Arctic warming and glacier thinning, it is possible that the glaciers characterised by the polythermal valley glacier landsystem will continue to transition to the geomorphological endpoint for Svalbard glaciers, represented by the small vanishing glacier landsystem. For example, although the vanishing glacier landsystem (Fig. 14) is largely based on Protektorbreen and Ferdinandbreen, it is worth noting that parts of the Scottbreen forefield share many of the key

Table 2
Summary and key characteristics of Svalbard glacier landsystems.

	Surge-type		Non-surge-type	
	Marine-terminating glacier (Fig. 11)	Land-terminating glacier (Fig. 12)	Polythermal valley glacier (Fig. 13)	Small vanishing glacier (Fig. 14)
Glacier size				
Glacier type	Typically, outlet or tributary glaciers in a larger glacier system.	Can be outlet or tributary glaciers from a larger system or individual valley glaciers.	Can be independent valley glaciers, tributaries of a larger system or icefield outlets.	Typically, cirque glaciers or smaller glaciers disconnected from larger accumulation areas.
Glacier hypsometry	Bottom heavy hypsometry.	Very bottom heavy or bottom heavy hypsometry.	Equidimensional to very bottom heavy hypsometry.	Very bottom heavy or bottom heavy hypsometry.
Key landforms	Glaciotectonic moraines are common in terrestrial and seafloor positions with low gradient debris flows on seafloor moraines.	Large glaciotectonic moraines mark the maximum extent of surge(s) and dam proglacial lakes (but not always).	Well defined lateral and (often, but not always) frontal moraines mark former maximum position and ice surface height.	Well defined lateral and terminal moraines mark former maximum position and ice surface height.
	CSRs and glacial lineations dominate the submarine and terrestrial environments.	CSRs are common in the forefield alongside often heavily crevassed glacier margins.	The inner forefield is dominated by active and inactive glaciofluvial outwash.	Thin debris drapes and supraglacial debris stripes originating from supraglacial positions dominate the forefield.
	Well-developed glaciofluvial outwash may be present on the terrestrial margin.	Well-developed glaciofluvial outwash may be present.	Inactive channels often trace the ice front, indicating frozen margins.	There is very limited meltwater activity with inactive meltwater channels representing past activity.
	Seafloor eskers can be long and extend from the position of subglacial meltwater portals.	Subglacial landforms such as flutes and eskers (including zig-zag eskers) dominate the forefield.	Streamlined terrain is common, with occasional well-preserved eskers.	Bedrock outcrops are common across the forefield and may separate ice masses.
	Retreat moraines on the seafloor but not in terrestrial positions.	Ice stagnation terrain and dead-ice is common.	Proglacial icings may be present adjacent to active meltwater channels.	Glacier fragmentins around bedrock outcrops as it thins and becomes disconnected from larger source areas.

characteristics (Fig. 6A). At Scottbreen's northern ice margin, supraglacial sediment drapes with debris stripes are becoming the dominant feature in the forefield, and active meltwater activity is much more spatially constrained than the other polythermal glacier examples. It is perhaps no surprise that Scottbreen is the next smallest glacier after Ferdinandbreen and Protektorbreen in these examples (Table 1), and it similarly has no larger accumulation area feeding it. We therefore suggest that the emerging geomorphological signature at Scottbreen may be an early sign of its transition towards a small vanishing glacier landsystem, and ultimately its terminal decline.

5.2. *Glacier sensitivity to climate change*

The Arctic is particularly sensitive to climate change and thus shifts in the global and regional climate will likely accelerate changes to glacier thermal regimes (Zhang et al., 2019, Marshall, 2021). One of the consequences in High-Arctic locations where many glaciers are polythermal is the phenomenon of small glaciers becoming colder as the climate warms. The enhanced mass loss associated with climate change will further drive glacier thinning and ultimately a shift into frozen bed conditions as the bed would no longer be at the pressure-melting point to sustain basal melt. This describes the situation where previously thicker, polythermal glaciers with some component of warm-based flow become too thin under warmer temperatures and thus become frozen to the bed and entirely cold throughout (e.g. Bælum and Benn, 2011; Małecki, 2013; Carrivick et al., 2023).

Glacier hypsometry can help to understand the impact of future warming on glacier thinning and thus transitions in thermal regime, particularly in smaller glaciers. HI were calculated for each glacier in this study, which describes the elevation distribution of the glacier surface. Different distributions, particularly in relation to the equilibrium line altitude (ELA), will have different sensitivities towards climate change and its impacts (McGrath et al., 2017). A glacier with more mass at lower elevations will be more sensitive to temperature increases due to the proportion of their mass below the ELA (Noël et al., 2020). Nearly all the glaciers analysed here trend towards a bottom-heavy or very bottom-heavy hypsometry (Table 1). Combined with the general low elevation and flat interiors of Svalbard glaciers, this makes them particularly susceptible to temperature increases associated with climate change (Noël et al., 2020). The low-lying glaciers in southern Svalbard are modelled to be some of the most vulnerable to climate warming due to the ELA rising above the hypsometry peak, resulting in zero accumulation-area ratios in the next decade (McGrath et al., 2017; Sass et al., 2017; Noël et al., 2020; van Pelt et al., 2021).

Hypsometrically-controlled melt-accelerated feedbacks will continue to drive glacier thinning, particularly at already vulnerable polythermal glaciers such as Scottbreen and where fragmentation from larger accumulation areas has occurred. Once already vulnerable glaciers become fragmented from any larger accumulation area they become even more vulnerable to mass loss (Paul et al., 2004; Jiskoot et al., 2009; Jiskoot and Mueller, 2012; Davies et al., 2022, 2024). Fragmentation of glacier ice is a characteristic that is easy to detect both in the field and remotely, thus these landsystems also provide insight into the condition of glaciers that are transitioning into a terminal state. Ferdinandbreen appears to be quite far along this journey, with the glacier already heavily fragmented and entirely disconnected from its past larger accumulation area. It is not necessary to look far for an example of Ferdinandbreen's likely end-state in the not-too-distant future: the neighbouring cirque to the south is almost completed deglaciated, save for a small remnant of Elsabreen preserved under the backwall (Fig. 15).

6. Conclusions

Here, we present four glacier landsystems for Svalbard based on the geomorphology at 11 glaciers in south and northwest Spitsbergen. The

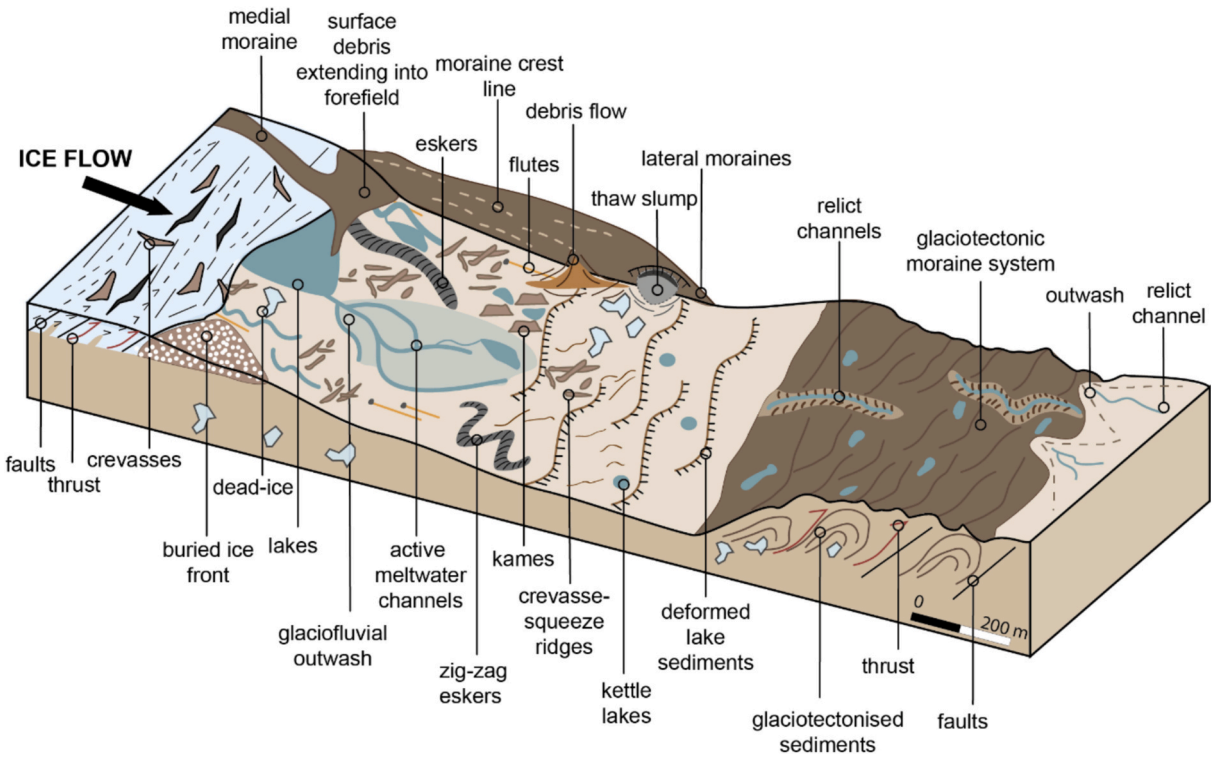

Fig. 12. Land-terminating surge-type glacier landsystem.

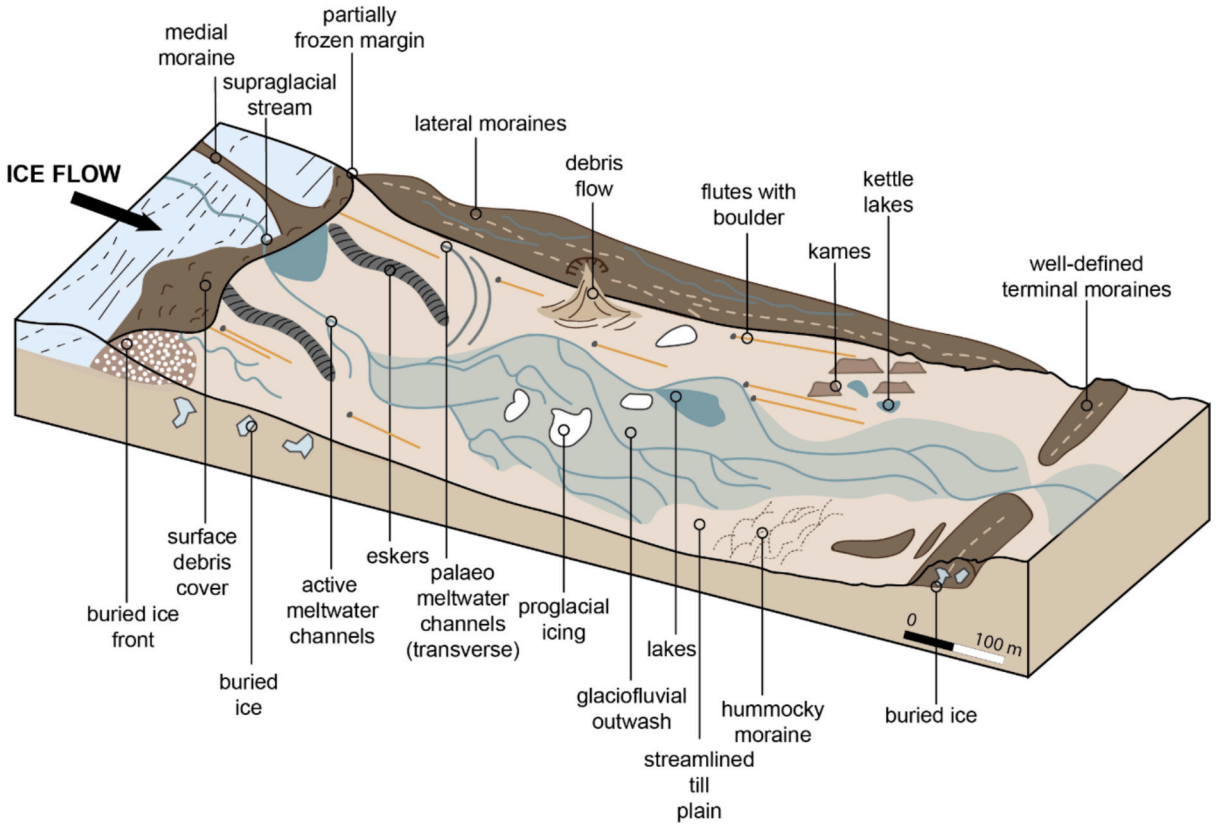

Fig. 13. Polythermal valley glacier landsystem.

landsystems represent a continuum of glacier dynamics encompassing marine- and land-terminating surge-type glaciers, polythermal valley glaciers with evidence of past dynamism, and small vanishing glaciers that are rapidly fragmenting and ultimately disappearing, representing the geomorphological endpoint for Svalbard glaciers. The surge-type glacier landsystems include both marine-terminating and land-

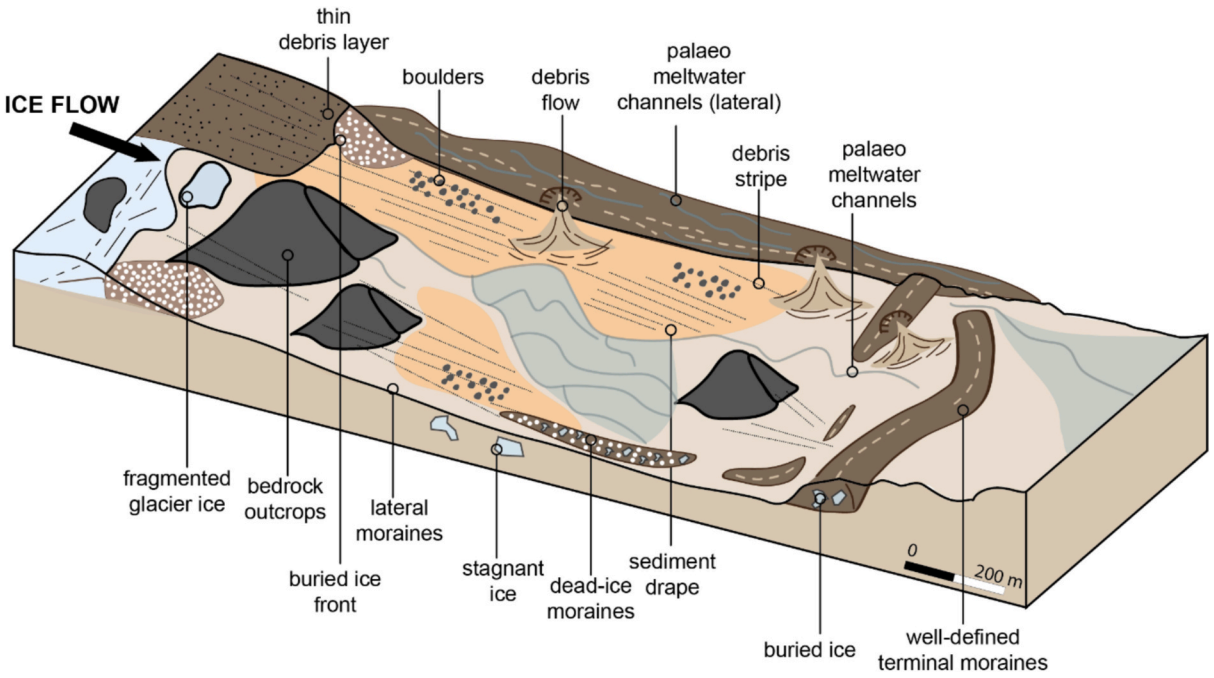

Fig. 14. Vanishing glacier landsystem.

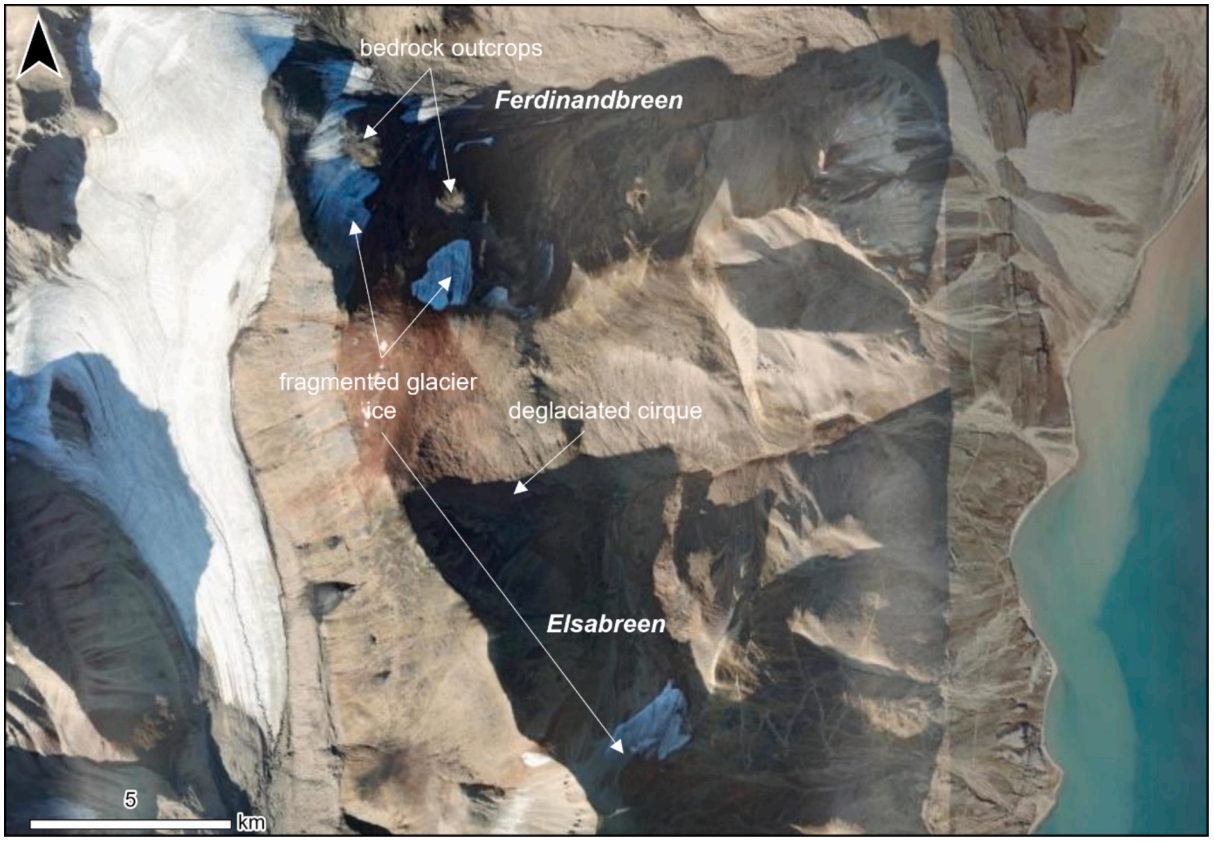

Fig. 15. The geomorphological endpoint for Svalbard glaciers illustrated by the almost deglaciated Elsabreen valley to the south and heavily fragmented and disconnected Ferdinandbreen to the north.

terminating examples, with key landforms present in both that provide a diagnostic link to processes that are active during surges - including CSRs and glaciotectonic moraine systems. Polythermal valley glaciers are characterised by ice-cored moraine systems, active meltwater systems and extensive glaciofluvial outwash, and the presence of sub-glacial bedforms indicative of warm-based conditions, such as flutes. The vanishing glacial landsystem represents an endpoint for Svalbard glaciers and is characterised by heavily fragmented and thin glacier ice,

extensive bedrock outcrops, thin supraglacial sediment drapes and limited meltwater activity. It is possible to identify evidence for transitions between landsystems, such as features indicating a more-dynamic, potentially surging past for polythermal valley glaciers that are currently largely inactive. There is also contemporary signs that some polythermal valley glaciers are starting to produce supraglacial-dominated forefields, few or no subglacial features and with only limited meltwater activity apparent, thus beginning that transition to becoming a vanishing glacier. The landsystem models presented here provide an important insight into the future of many small land-terminating glaciers on Svalbard under current climate conditions.

CRediT authorship contribution statement

Rebecca McCerery: Visualization, Validation, Project administration, Methodology, Investigation, Formal analysis, Data curation, Conceptualization, Writing – review & editing, Writing – original draft. **Bethan J. Davies:** Visualization, Resources, Methodology, Investigation, Formal analysis, Data curation, Conceptualization, Writing – original draft. **Harold Lovell:** Visualization, Resources, Methodology, Investigation, Formal analysis, Data curation, Conceptualization, Writing – original draft. **Rosalia Calvo-Ryan:** Investigation, Data curation, Writing – review & editing. **David A. Pearce:** Investigation, Funding acquisition, Data curation, Writing – review & editing. **Jakub Małecki:** Resources, Methodology, Investigation, Formal analysis, Data curation, Conceptualization, Writing – review & editing. **John Woodward:** Visualization, Supervision, Resources, Project administration, Methodology, Investigation, Funding acquisition, Writing – review & editing.

Declaration of competing interest

The authors declare that they have no known competing financial interests or personal relationships that could have appeared to influence the work reported in this paper.

Acknowledgements

This work was supported by Northumbria University and Svalbard Integrated Arctic Earth Observing System (SIOS) Access Fund under Grant SIOS Access 2020_0009 awarded to DP. All authors would like to thank the crew of Ulla Rinman, whose logistical support and valuable insight resulted in a successful field season. Fieldwork in Petuniabukta benefitted from funding from the University of Portsmouth and logistical support from Adam Mickiewicz University, including use of the Petuniabukta Polar Station.

Data availability

Data will be made available on request.

References

Aradóttir, N., Ingólfsson, Ó., Noormets, R., Benediktsson, Í.Ö., Ben-Yehoshua, D., Håkansson, L., Schomacker, A., 2019. Glacial geomorphology of Trygghamna, western Svalbard-Integrating terrestrial and submarine archives for a better understanding of past glacial dynamics. Geomorphology 344, 75–89. https://doi.org/10.1016/j.geomorph.2019.07.007.

Bælum, K., Benn, D.I., 2011. Structure and drainage system of a small valley glacier (Tellbreen, Svalbard), investigated by ground penetrating radar. Cryosphere 5, 139–149. https://doi.org/10.5194/tc-5-139-2011.

Benn, D.I., Kristensen, L., Gulley, J.D., 2009. Surge propagation constrained by a persistent subglacial conduit, Bakaninbreen–Paulabreen, Svalbard. Ann. Glaciol. 50 (52), 81–86. https://doi.org/10.3189/172756409789624337.

Benn, D.I., Kirkbride, M.P., Owen, L.A., Brazier, V., 2014. Glaciated valley landsystems. In: Glacial landsystems. Routledge, pp. 372–406.

Ben-Yehoshua, D., Aradóttir, N., Farnsworth, W.R., Benediktsson, Í.Ö., Ingólfsson, Ó., 2023. Formation of crevasse-squeeze ridges at Trygghamna, Svalbard. Earth Surf. Process. Landf. 48 (12), 2334–2348. https://doi.org/10.1002/esp.5631.

Björnsson, H., Pálsson, F., Sigurðsson, O., Flowers, G.E., 2003. Surges of glaciers in Iceland. Ann. Glaciol. 36, 82–90. https://doi.org/10.3189/172756403781816365.

Błaszczyk, M., Jania, J.A., and Hagen, J.O., (2009) 'Tidewater glaciers of Svalbard: recent changes and estimates of calving fluxes' Pol. Polar Res., (2), pp.85–102.

Boulton, G.S., 1972. Modern arctic glaciers as depositional models for former ice sheets. J. Geol. Soc. Lond. 128, 361–393. https://doi.org/10.1144/gsjgs.128.4.0361.

Boulton, G.S., Van der Meer, J.J.M., Hart, J., Beets, D., Ruegg, G.H.J., Van der Wateren, F.M., Jarvis, J., 1996. Till and moraine emplacement in a deforming bed surge—an example from a marine environment. Quat. Sci. Rev. 15 (10), 961–987. https://doi.org/10.1016/0277-3791(95)00091-7.

Boulton, G.S., Van der Meer, J.J.M., Beets, D.J., Hart, J.K., Ruegg, G.H.J., 1999. The sedimentary and structural evolution of a recent push moraine complex: Holmströmbreen, Spitsbergen. Quat. Sci. Rev. 18 (3), 339–371. https://doi.org/10.1016/S0277-3791(98)00068-7.

Carrivick, J.L., Smith, M.W., Sutherland, J.L., Grimes, M., 2023. Cooling glaciers in a warming climate since the Little Ice Age at Qaanaaq, northwest Kalaallit Nunaat (Greenland). Earth Surf. Process. Landf. 48 (13), 2446–2462. https://doi.org/10.1002/esp.5638.

Chandler, B.M., Lovell, H., Boston, C.M., Lukas, S., Barr, I.D., Benediktsson, Í.Ö., Benn, D. I., Clark, C.D., Darvill, C.M., Evans, D.J., Ewertowski, M.W., 2018. Glacial geomorphological mapping: a review of approaches and frameworks for best practice. Earth-Sci. Rev. 185, 806–846. https://doi.org/10.1016/j.earscirev.2018.07.015.

Chandler, B.M., Evans, D.J., Chandler, S.J., Ewertowski, M.W., Lovell, H., Roberts, D.H., Schaefer, M., Tomczyk, A.M., 2020. The glacial landsystem of Fjallsjökull, Iceland: Spatial and temporal evolution of process-form regimes at an active temperate glacier. Geomorphology 361, 107192. https://doi.org/10.1016/j.geomorph.2020.107192.

Christoffersen, P., Piotrowski, J.A., Larsen, N.K., 2005. Basal processes beneath an Arctic glacier and their geomorphic imprint after a surge, Elisebreen. Svalbard. Quat. Res. 64 (2), 125–137. https://doi.org/10.1016/j.yqres.2005.05.009.

Clayton, L. and Moran, S.R. (1974) A glacial process-form model. In: Glacial Geomorphology: A Proceedings Volume of the Fifth Annual Geomorphology Symposia Series, Held at Binghamton New York September 26–28, 1974 (89–119). Dordrecht: Springer Netherlands.

Croot, D.G., 1988. Glaciotectonics and surging glaciers: a correlation based on Vestspitsbergen, Svalbard, Norway. In: Croot, D.G. (Ed.), Glaciotectonics: Forms and Processes. Balkema, Rotterdam, pp. 33–47.

Davies, B., Bendle, J., Carrivick, J., McNabb, R., McNeil, C., Pelto, M., Campbell, S., Holt, T., Ely, J., Markle, B., 2022. Topographic controls on ice flow and recession for Juneau Icefield (Alaska/British Columbia). Earth Surf. Process. Landf. 47 (9), 2357–2390. https://doi.org/10.1002/esp.5383.

Davies, B., McNabb, R., Bendle, J., Carrivick, J., Ely, J., Holt, T., Markle, B., McNeil, C., Nicholson, L., Pelto, M., 2024. Accelerating glacier volume loss on Juneau Icefield driven by hypsometry and melt-accelerating feedbacks. Nat. Commun. 15 (1), 5099. https://doi.org/10.1038/s41467-024-49269-y.

Davies, B.J., Glasser, N.F., Carrivick, J.L., Hambrey, M.J., Smellie, J.L., Nývlt, D., 2013. Landscape evolution and ice-sheet behaviour in a semi-arid polar environment: James Ross Island, NE Antarctic Peninsula. Geol. Soc. Lond. Spec. Publ. 381 (1), 353–395. https://doi.org/10.1144/SP381.1.

Descamps, S., Aars, J., Fuglei, E., Kovacs, K.M., Lydersen, C., Pavlova, O., Pedersen, Å.Ø., Ravolainen, V., Strøm, H., 2017. Climate change impacts on wildlife in a High Arctic archipelago–Svalbard, Norway. Glob. Chang. Biol. 23 (2), 490–502. https://doi.org/10.1111/gcb.13381.

Ding, M., Wang, S., Sun, W., 2018. Decadal climate change in Ny-Ålesund, Svalbard, a representative area of the Arctic. Condens. Matter 3 (2), 12. https://doi.org/10.3390/condmat3020012.

Dowdeswell, J., Hamilton, G., Hagen, J., 1991. The duration of the active phase on surge-type glaciers: contrasts between Svalbard and other regions. J. Glaciol. 37 (127), 388–400. https://doi.org/10.3189/S0022143000005827.

Drange, H., Dokken, T., Furevik, T., Gerdes, R., Berger, W., Nesje, A., Orvik, K.A., Skagseth, Ø., 2005. The Nordic Seas: an overview. In: Drange, H., Dokken, T., Furevik, T., Gerdes, R., Berger, W. (Eds.), The Nordic Seas: An Integrated Perspective, 158. Am. Geophys. Union, p. 1.

Eckerstorfer, M., Christiansen, H.H., 2011. The "High Arctic maritime snow climate" in central Svalbard. Arct. Antarct. Alp. Res. 43 (1), 11–21. https://doi.org/10.1657/1938-4246-43.1.11.

Ely, J.C., Graham, C., Barr, I.D., Rea, B.R., Spagnolo, M., Evans, J., 2017. Using UAV acquired photography and structure from motion techniques for studying glacier landforms: application to the glacial flutes at Isfallsglaciären. Earth Surf. Process. Landf. 42 (6), 877–888. https://doi.org/10.1002/esp.4044.

England, M.R., Eisenman, I., Lutsko, N.J., Wagner, T.J., 2021. The recent emergence of Arctic amplification. Geophys. Res. Lett. 48 (15), e2021GL094086. https://doi.org/10.1029/2021GL094086.

Evans, D.J., 2009. Controlled moraines: origins, characteristics and palaeoglaciological implications. Quat. Sci. Rev. 28 (3–4), 183–208. https://doi.org/10.1016/j.quascirev.2008.10.024.

Evans, D.J. (2014) 'Introduction to glacial landsystems'. In: Evans, D.J. Glacial landsystems (1–11). Routledge: Oxon.

Evans, D.J., Rea, B.R., 1999. Geomorphology and sedimentology of surging glaciers: a land-systems approach. Ann. Glaciol. 28, 75–82. https://doi.org/10.3189/172756499781821823.

Evans, D.J. and Rea, B.R. (2014) 'Surging glacier landsystem' In: Glacial Landsystems (pp.259–288). Routledge: Oxon.

Evans, D.J., Twigg, D.R., 2002. The active temperate glacial landsystem: a model based on Breiðamerkurjökull and Fjallsjökull, Iceland. Quat. Sci. Rev. 21 (20−22), 2143–2177. https://doi.org/10.1016/S0277-3791(02)00019-7.

Evans, D.J., Twigg, D.R., Rea, B.R., Orton, C., 2009. Surging glacier landsystem of Tungnaárjökull, Iceland. J. Maps 5 (1), 134–151. https://doi.org/10.4113/jom.2009.1064.

Evans, D.J., Strzelecki, M., Milledge, D.G., Orton, C., 2012. Hørbyebreen polythermal glacial landsystem, Svalbard. J. Maps 8 (2), 146–156. https://doi.org/10.1080/17445647.2012.680776.

Evans, D.J., Ewertowski, M., Roberts, D.H., Tomczyk, A.M., 2022. The historical emergence of a geometric and sinuous ridge network at the Hørbyebreen polythermal glacier snout, Svalbard and its use in the interpretation of ancient glacial landforms. Geomorphology 406, 108213. https://doi.org/10.1016/j.geomorph.2022.108213.

Ewertowski, M., 2014. Recent transformations in the high-Arctic glacier landsystem, Ragnarbreen, Svalbard. Geogr. Ann. Ser. B 96 (3), 265–285. https://doi.org/10.1111/geoa.12049.

Ewertowski, M.W., Tomczyk, A.M., 2020. Reactivation of temporarily stabilized ice-cored moraines in front of polythermal glaciers: Gravitational mass movements as the most important geomorphological agents for the redistribution of sediments (a case study from Ebbabreen and Ragnarbreen, Svalbard). Geomorphology 350, 106952. https://doi.org/10.1016/j.geomorph.2019.106952.

Ewertowski, M.W., Evans, D.J., Roberts, D.H., Tomczyk, A.M., Ewertowski, W., Pleksot, K., 2019. Quantification of historical landscape change on the foreland of a receding polythermal glacier, Hørbyebreen. Svalbard. Geomorphology 325, 40–54. https://doi.org/10.1016/j.geomorph.2018.09.027.

Farnsworth, W.R., Ingólfsson, Ó., Retelle, M., Schomacker, A., 2016. Over 400 previously undocumented Svalbard surge-type glaciers identified. Geomorphology 264, 52–60. https://doi.org/10.1016/j.geomorph.2016.03.025.

Farnsworth, W.R., Ingólfsson, Ó., Noormets, R., Allaart, L., Alexanderson, H., Henriksen, M., Schomacker, A., 2017. Dynamic Holocene glacial history of St. Jonsfjorden, Svalbard. Boreas 46 (3), 585–603. https://doi.org/10.1111/bor.12269.

Farnsworth, W.R., Allaart, L., Ingólfsson, Ó., Alexanderson, H., Forwick, M., Noormets, R., Retelle, M., Schomacker, A., 2020. Holocene glacial history of Svalbard: Status, perspectives and challenges. Earth Sci. Rev. 208, 103249. https://doi.org/10.1016/j.earscirev.2020.103249.

Flink, A.E., Noormets, R., Kirchner, N., Benn, D.I., Luckman, A., Lovell, H., 2015. The evolution of a submarine landform record following recent and multiple surges of Tunabreen glacier, Svalbard. Quat. Sci. Rev. 108, 37–50. https://doi.org/10.1016/j.quascirev.2014.11.006.

French, M.H. 2007 The periglacial environment. Third edition. Chichester, U.K. and Hoboken, New Jersey John Wiley & Sons. pp.458.

Furbish, D.J., Andrews, J.T., 1984. The use of hypsometry to indicate long-term stability and response of valley glaciers to changes in mass transfer. J. Glaciol. 30 (105), 199–211. https://doi.org/10.3189/S0022143000005931.

Geyman, E.C., van Pelt, W.J.J., Maloof, A.C., Aas, H.F., Kohler, J., 2022. Historical glacier change on Svalbard predicts doubling of mass loss by 2100. Nature 601 (7893), 374–379. https://doi.org/10.1038/s41586-021-04314-4.

Glasser, N.F. and Hambrey, M.J. (2005) 'Ice-marginal terrestrial landsystems: Svalbard polythermal glaciers' In: Glacial landsystems (65–88). Routledge.

Hagen, J.O., 1988. Glacier surge in Svalbard with examples from Usherbreen. Norsk Geografisk Tidsskrift - Norwegian J. Geogr. 42 (4), 203–213. https://doi.org/10.1080/00291958808552202.

Hagen, J.O., Liestøl, O., Roland, E., Jørgensen, T., 1993. Glacier atlas of Svalbard and jan Mayen. Norwegian Polar Institute Meddelelser 129, 1–141.

Hagen, J.O., Kohler, J., Melvold, K., Winther, J.G., 2003. Glaciers in Svalbard: mass balance, runoff and freshwater flux. Polar Res. 22 (2), 145–159. https://doi.org/10.1111/j.1751-8369.2003.tb00104.x.

Hald, M., Dahlgren, T., Olsen, T.E., Lebesbye, E., 2001. Late holocene palaeoceanography in van Mijenfjorden, svalbard. Polar Res. 20 (1), 23–35. https://doi.org/10.3402/polar.v20i1.6497.

Hart, J.K., Watts, R.J., 1997. A comparison of the styles of deformation associated with two recent push moraines, South Van Keulenfjorden, Svalbard. Earth Surf. Process. Landf. 22 (12), 1089–1107. https://doi.org/10.1002/(SICI)1096-9837(199712)22:12%3C1089::AID-ESP804%3E3.0.CO;2-8.

Hättestrand, C., Stroeven, A.P., 2002. A relict landscape in the Centre of Fennoscandian glaciation: Geomorphological evidence of minimal Quaternary glacial erosion. Geomorphology 44 (1–2), 127–143. https://doi.org/10.1016/S0169-555X(01)00149-0.

Holmlund, E.S., 2021. Aldegondabreen glacier change since 1910 from structure-from-motion photogrammetry of archived terrestrial and aerial photographs: Utility of a historic archive to obtain century-scale Svalbard glacier mass losses. J. Glaciol. 67 (261), 107–116. https://doi.org/10.1017/jog.2020.89.

Ingólfsson, Ó., Benediktsson, Í.Ö., Schomacker, A., Kjær, K.H., Brynjólfsson, S., Jónsson, S.A., Korsgaard, N.J., Johnson, M.D., 2016. Glacial geological studies of surge-type glaciers in Iceland—Research status and future challenges. Earth Sci. Rev. 152, 37–69. https://doi.org/10.1016/j.earscirev.2015.11.008.

James, M.R., Chandler, J.H., Eltner, A., Fraser, C., Miller, P.E., Mills, J.P., Noble, T., Robson, S., Lane, S.N., 2019. Guidelines on the use of the structure-from-motion photogrammetry in geomorphic research. Earth Surf. Process. Landf. 44, 2081–2084. https://doi.org/10.1002/esp.4637.

Jiskoot, H., Mueller, M.S., 2012. Glacier fragmentation effects on surface energy balance and runoff: field measurements and distributed modelling. Hydrol. Process. 26 (12), 1861–1875. https://doi.org/10.1002/hyp.9288.

Jiskoot, H., Curran, C.J., Tessler, D.L., Shenton, L.R., 2009. Changes in Clemenceau Icefield and Chaba Group glaciers, Canada, related to hypsometry, tributary detachment, length–slope and area–aspect relations. Ann. Glaciol. 50 (53), 133–143. https://doi.org/10.3189/172756410790595796.

Jónsson, S.A., Schomacker, A., Benediktsson, Í.Ö., Ingólfsson, Ó., Johnson, M.D., 2014. The drumlin field and the geomorphology of the Múlajökull surge-type glacier, Central Iceland. Geomorphology 207, 213–220. https://doi.org/10.1016/j.geomorph.2013.11.007.

Kääb, A., Bazilova, V., Leclercq, P.W., Mannerfelt, E.S., Strozzi, T., 2023. Global clustering of recent glacier surges from radar backscatter data, 2017–2022. J. Glaciol. 69 (277), 1515–1523. https://doi.org/10.1017/jog.2023.35.

Kjær, K.H., Korsgaard, N.J., Schomacker, A., 2008. Impact of multiple glacier surges—a geomorphological map from Brúarjökull, East Iceland. J. Maps 4 (1), 5–20. https://doi.org/10.4113/jom.2008.91.

Koch, M., Seehaus, T., Friedl, P., Braun, M., 2023. Automated Detection of Glacier Surges from Sentinel-1 Surface Velocity Time Series—an example from Svalbard. Remote Sens. 15 (6), 1545. https://doi.org/10.3390/rs15061545.

Kochtitzky, W., Copland, L., 2022. Retreat of northern hemisphere marine-terminating glaciers, 2000–2020. Geophys. Res. Lett. 49 (3), e2021GL096501. https://doi.org/10.1029/2021GL096501.

Krawczyk, W.E., Bartoszewski, S.A., 2008. Crustal solute fluxes and transient carbon dioxide drawdown in the Scottbreen Basin, Svalbard in 2002. J. Hydrol. 362 (3–4), 206–219. https://doi.org/10.1016/j.jhydrol.2008.08.025.

Kristensen, L., Benn, D.I., 2012. A surge of the glaciers Skobreen–Paulabreen, Svalbard, observed by time-lapse photographs and remote sensing data. Polar Res. 31 (1). https://doi.org/10.3402/polar.v31i0.11106.

Kristensen, L., Benn, D.I., Hormes, A., Ottesen, D., 2009. Mud aprons in front of Svalbard surge moraines: evidence of subglacial deforming layers or proglacial glaciotectonics? Geomorphology 111 (3–4), 206–221. https://doi.org/10.1016/j.geomorph.2009.04.022.

Krüger, J., 1994. Glacial processes, sediments, landforms, and stratigraphy in the terminus region of Myrdalsjökull, Iceland: two interdisciplinary case studies. Folia Geogr. Dan. 21, 1–233.

Krüger, J., Kjær, K.H. and Schomacker, A. 2010 '7 Dead-Ice Environments: a Landsystems Model for a Debris-Charged, Stagnant Lowland Glacier margin, Kötlujökull' Developments in quaternary sciences, 13, pp.105–126, https://doi.org/10.1016/S1571-0866(09)01307-4.

Larsen, E., Lysså, A., Rubensdotter, L., Farnsworth, W.R., Jensen, M., Nadeau, M.J., Ottesen, D., 2018. Lateglacial and Holocene glacier activity in the Van Mijenfjorden area, western Svalbard. Arktos 4, 1–21. https://doi.org/10.1007/s41063-018-0042-2.

Le Heron, D.P., Kettler, C., Davies, B.J., Scharfenberg, L., Eder, L., Ketterman, M., Griesmeier, G.E., Quinn, R., Chen, X., Vandyk, T., Busfield, M.E., 2022. Rapid geomorphological and sedimentological changes at a modern Alpine ice margin: lessons from the Gepatsch Glacier, Tirol, Austria. J. Geol. Soc. 179 (3), jgs2021-052. https://doi.org/10.1144/jgs2021-052.

Lønne, I., 2016. A new concept for glacial geological investigations of surges, based on High-Arctic examples (Svalbard). Quat. Sci. Rev. 132, 74–100. https://doi.org/10.1016/j.quascirev.2015.11.009.

Lovell, H., Boston, C.M., 2017. Glacitectonic composite ridge systems and surge-type glaciers: an updated correlation based on Svalbard, Norway. Arktos 3, 1–16. https://doi.org/10.1007/s41063-017-0028-5.

Lovell, H., Fleming, E.J., 2023. Structural evolution during a surge in the Paulabreen glacier system, Svalbard. J. Glaciol. 69 (273), 141–152. https://doi.org/10.1017/jog.2022.53.

Lovell, H., Fleming, E.J., Benn, D.I., Hubbard, B., Lukas, S., Naegeli, K., 2015. Former dynamic behaviour of a cold-based valley glacier on Svalbard revealed by basal ice and structural glaciology investigations. J. Glaciol. 61 (226), 309–328. https://doi.org/10.3189/2015JoG14J120.

Lovell, H., Benn, D.I., Lukas, S., Spagnolo, M., Cook, S.J., Swift, D.A., Clark, C.D., Yde, J. C., Watts, T., 2018a. Geomorphological investigation of multiphase glacitectonic composite ridge systems in Svalbard. Geomorphology 300, 176–188. https://doi.org/10.1016/j.geomorph.2017.10.024.

Lovell, H., Benn, D.I., Lukas, S., Ottesen, D., Luckman, A., Hardiman, M., Barr, I.D., Boston, C.M., Sevestre, H., 2018b. Multiple late Holocene surges of a High-Arctic tidewater glacier system in Svalbard. Quat. Sci. Rev. 201, 162–185. https://doi.org/10.1016/j.quascirev.2018.10.024.

Małecki, J., 2013. Elevation and volume changes of seven Dickson Land glaciers, Svalbard, 1960–1990–2009. Polar Res. 32 (1), 18400.

Małecki, J., 2016. Accelerating retreat and high-elevation thinning of glaciers in Central Spitsbergen. Cryosphere 10, 1317–1329. https://doi.org/10.5194/tc-10-1317-2016.

Małecki, J., Lovell, H., Ewertowski, W., Górski, Ł., Kurczaba, T., Latos, B., Miara, M., Piniarska, D., Płocieniczak, J., Sowada, T., Spiralski, M., 2018. The glacial landsystem of a tropical glacier: Charquini Sur, Bolivian Andes. Earth Surf. Process. Landf. 43 (12), 2584–2602. https://doi.org/10.1002/esp.4417.

Mallinson, L., Swift, D.A., Sole, A., 2019. Proglacial icings as indicators of glacier thermal regime: ice thickness changes and icing occurrence in Svalbard. Geogr. Ann. Ser. B 101 (4), 334–349. https://doi.org/10.1080/04353676.2019.1670952.

Mangerud, J.A.N., Landvik, J.Y., 2007. Younger Dryas cirque glaciers in western Spitsbergen: smaller than during the Little Ice Age. Boreas 36 (3), 278–285. https://doi.org/10.1111/j.1502-3885.2007.tb01250.x.

Mannerfelt, E.S., Hodson, A.J., Håkansson, L., Lovell, H., 2024a. Dynamic LIA advances hastened the demise of small valley glaciers in Central Svalbard. Arctic Sci. 1–19. https://doi.org/10.1139/as-2024-0024.

Mannerfelt, E.S., Schellenberger, T., Kääb, A., 2024b. Tracking glacier surge evolution using interferometric SAR coherence – examples from Svalbard. J. Glaciol. 71, e43. https://doi.org/10.1017/jog.2025.27.

Marshall, S.J., 2021. Regime shifts in glacier and ice sheet response to climate change: examples from the Northern Hemisphere. Front. Clim. 3, 702585. https://doi.org/10.3389/fclim.2021.702585.

Martín-Moreno, R., Alvarez, Allende, Hagen, J.O., 2017. Little Ice Age'glacier extent and subsequent retreat in Svalbard archipelago. The Holocene 27 (9), 1379–1390. https://doi.org/10.1177/0959683617693904.

McCerery, R., Davies, B.J., Lovell, H., Pearce, D.A., Calvo-Ryan, R., Małecki, J., Woodward, J., 2024. Terrestrial glacial geomorphology of surge-type and non-surge-type glaciers on Svalbard. J. Maps 20 (1), 2362277. https://doi.org/10.1080/17445647.2024.2362277.

McGrath, D., Sass, L., O'Neel, S., Arendt, A., Kienholz, C., 2017. Hypsometric control on glacier mass balance sensitivity in Alaska and Northwest Canada. Earth's Future 5 (3), 324–336. https://doi.org/10.1002/2016EF000479.

Morris, A., Moholdt, G., Gray, L., 2020. Spread of Svalbard glacier mass loss to Barents Sea margins revealed by CryoSat-2. J. Geophys. Res. Earth Surf. 125 (8), e2019JF005357. https://doi.org/10.1029/2019JF005357.

Murray, T., Dowdeswell, J.A., Drewry, D.J., Frearson, I., 1998. Geometric evolution and ice dynamics during a surge of Bakaninbreen, Svalbard. J. Glaciol. 44 (147), 263–272. https://doi.org/10.3189/S0022143000002604.

Murray, T., Strozzi, T., Luckman, A., Jiskoot, H., Christakos, P., 2003. Is there a single surge mechanism? Contrasts in dynamics between glacier surges in Svalbard and other regions. J. Geophys. Res. Solid Earth 108 (B5), 2237. https://doi.org/10.1029/2002JB001906.

Noël, B., Jakobs, C.L., Van Pelt, W.J.J., Lhermitte, S., Wouters, B., Kohler, J., Hagen, J.O., Luks, B., Reijmer, C.H., Van de Berg, W.J., van den Broeke, M.R., 2020. Low elevation of Svalbard glaciers drives high mass loss variability. Nat. Commun. 11 (1), 4597. https://doi.org/10.1038/s41467-020-18356-1.

Nordli, Ø., Wyszyński, P., Gjelten, H., Isaksen, K., Łupikasza, E., Niedźwiedź, T., Przybylak, R., 2020. Revisiting the Extended Svalbard Airport Monthly Temperature Series, and the Compiled Corresponding Daily Series, pp. 1898–2018.

Nuth, C., Kohler, J., König, M., Von Deschwanden, A., Hagen, J.O., Kääb, A., Moholdt, G., Pettersson, R., 2013. Decadal changes from a multi-temporal glacier inventory of Svalbard. Cryosphere 7 (5), 1603–1621. https://doi.org/10.5194/tc-7-1603-2013.

Osika, A., Jania, J., 2024. Geomorphological and historical records of the surge-type behaviour of Hansbreen (Svalbard). Ann. Glaciol. 1–18. https://doi.org/10.1017/aog.2024.32.

Ottesen, D., Dowdeswell, J.A., 2006. Assemblages of submarine landforms produced by tidewater glaciers in Svalbard. J. Geophys. Res. Earth 111 (F1). https://doi.org/10.1029/2005JF000330.

Ottesen, D., Dowdeswell, J.A., Benn, D.I., Kristensen, L., Christiansen, H.H., Christensen, O., Hansen, L., Lebesbye, E., Forwick, M., Vorren, T.O., 2008. Submarine landforms characteristic of glacier surges in two Spitsbergen fjords. Quat. Sci. Rev. 27 (15–16), 1583–1599. https://doi.org/10.1016/j.quascirev.2008.05.007.

Ottesen, D., Dowdeswell, J.A., Bellec, V.K., Bjarnadóttir, L.R., 2017. The geomorphic imprint of glacier surges into open-marine waters: examples from eastern Svalbard. Mar. Geol. 392, 1–29. https://doi.org/10.1016/j.margeo.2017.08.007.

Paul, F., Kääb, A., Maisch, M., Kellenberger, T., Haeberli, W., 2004. Rapid disintegration of Alpine glaciers observed with satellite data. Geophys. Res. Lett. 31 (21). https://doi.org/10.1029/2004GL020816.

Philipps, W., Briner, J.P., Gislefoss, L., Linge, H., Koffman, T., Fabel, D., Xu, S., Hormes, A., 2017. Late Holocene glacier activity at inner Hornsund and Scottbreen, southern Svalbard. J. Quat. Sci. 32 (4), 501–515. https://doi.org/10.1002/jqs.2944.

Porter, C., et al., 2023. ArcticDEM, Version 4.1. Available at. https://doi.org/10.7910/DVN/3VDC4W. *Harvard Dataverse*, V1, [Accessed: 30/01/2024].

Rachlewicz, G., Szczuciński, W., Ewertowski, M., 2007. Post-'Little Ice Age' retreat rates of glaciers around Billefjorden in Central Spitsbergen, Svalbard. Pol. Polar Res. 3, 159–186.

Rea, B.R., Evans, D.J., 2011. An assessment of surge-induced crevassing and the formation of crevasse squeeze ridges. J. Geophys. Res. 116 (F4). https://doi.org/10.1029/2011JF001970.

RGI 7.0 Consortium (2023) Randolph Glacier Inventory - A Dataset of Global Glacier Outlines, Version 7.0. Boulder, Colorado USA. NSIDC: National Snow and Ice Data Center. Online access: doi:https://doi.org/10.5067/f6jmovy5navz.

Roberson, S., Hubbard, B., Coulson, H.R., Boomer, I., 2011. Physical properties and formation of flutes at a polythermal valley glacier: midre lovénbreen, Svalbard. Geogr. Ann. Ser. B 93 (2), 71–88. https://doi.org/10.1111/j.1468-0459.2011.00420.x.

Rootes, C.M., Clark, C.D., 2022. On the expression and distribution of glacial trimlines: a case study of Little Ice Age trimlines on Svalbard. E&G Quat. Sci. J. 71 (1), 111–122. https://doi.org/10.5194/egqsj-71-111-2022.

Russell, A.J., Knight, P.G., and Van Dijk, T.A.G.P. 2001 'Glacier surging as a control on the development of proglacial, fluvial landforms and deposits, Skeiðarársandur, Iceland' Glob. Planet. Chang., 28(1–4), pp.163-174, https://doi.org/10.1016/S0921-8181(00)00071-0.

Sass, L.C., Loso, M.G., Geck, J., Thoms, E.E., Mcgrath, D., 2017. Geometry, mass balance and thinning at Eklutna Glacier, Alaska: an altitude-mass-balance feedback with implications for water resources. J. Glaciol. 63 (238), 343–354. https://doi.org/10.1017/jog.2016.146.

Schomacker, A., Kjær, K.H., 2008. Quantification of dead-ice melting in ice-cored moraines at the high-Arctic glacier Holmströmbreen, Svalbard. Boreas 37 (2), 211–225. https://doi.org/10.1111/j.1502-3885.2007.00014.x.

Schomacker, A., Benediktsson, Í.Ö., Ingólfsson, Ó., 2014. The Eyjabakkajökull glacial landsystem, Iceland: geomorphic impact of multiple surges. Geomorphology 218, 98–107. https://doi.org/10.1016/j.geomorph.2013.07.005.

Sevestre, H., Benn, D.I., 2015. Climatic and geometric controls on the global distribution of surge-type glaciers: implications for a unifying model of surging. J. Glaciol. 61 (228), 646–662. https://doi.org/10.3189/2015JoG14J136.

Sharp, M., 1985. "Crevasse-fill" ridges—a landform type characteristic of surging glaciers? Geogr. Ann. Ser. B 67 (3–4), 213–220. https://doi.org/10.1080/04353676.1985.11880147.

Sharp, M., 1988. Surging glaciers: geomorphic effects. Prog. Phys. Geogr. 12 (4), 533–559. https://doi.org/10.3189/S0022143000008522.

Sund, M., 2006. A surge of Skobreen, Svalbard. Polar Res. 25 (2), 115–122. https://doi.org/10.3402/polar.v25i2.6241.

Tonkin, T.N., Midgley, N.G., Cook, S.J., Graham, D.J., 2016. Ice-cored moraine degradation mapped and quantified using an unmanned aerial vehicle: a case study from a polythermal glacier in Svalbard. Geomorphology 258, 1–10. https://doi.org/10.1016/j.geomorph.2015.12.019.

van der Meer, J.J., 2004. Spitsbergen push moraines: including a translation of K. Gripp: glaciologische und geologische ergebnisse der hamburgischen spitzbergen-expedition 1927, 4. Elsevier.

van Pelt, W.J., Schuler, T.V., Pohjola, V.A., Pettersson, R., 2021. Accelerating future mass loss of Svalbard glaciers from a multi-model ensemble. J. Glaciol. 67 (263), 485–499. https://doi.org/10.1017/jog.2021.2.

van Pelt, W.J.J., Oerlemans, J., Reijmer, C.H., Pohjola, V.A., Pettersson, R., van Angelen, J.H., 2012. Simulating melt, runoff and refreezing on Nordenskiöldbreen, Svalbard, using a coupled snow and energy balance model. Cryosphere 6, 641–659. https://doi.org/10.5194/tc-6-641-2012.

Vickers, H., Malnes, E., Eckerstorfer, M., 2022. A synthetic aperture radar based method for long term monitoring of seasonal snowmelt and wintertime rain-on-snow events in Svalbard. Front. Earth Sci. 10, 868945. https://doi.org/10.3389/feart.2022.868945.

Woodward, J., Murray, T., McCaig, A., 2002. Formation and reorientation of structure in the surge-type glacier Kongsvegen, Svalbard. Journal. Q. 17 (3), 201–209. https://doi.org/10.1002/jqs.673.

Woodward, J., Murray, T., Clark, R.A., Stuart, G.W., 2003. Glacier surge mechanisms inferred from ground-penetrating radar: Kongsvegen, Svalbard. J. Glaciol. 49 (167), 473–480. https://doi.org/10.3189/172756503781830458.

Yde, J.C., Knudsen, N.T., 2007. 20th-century glacier fluctuations on Disko Island (Qeqertarsuaq), Greenland. Ann. Glaciol. 46, 209–214. https://doi.org/10.3189/172756407782871558.

Zagórski, P., Gajek, G., Demczuk, P., 2012. The influence of glacier systems of polar catchments on the functioning of the coastal zone (Recherchefjorden, Svalbard). Zeitschrift fur Geomorphologie-Supplementband 56 (1), 101. https://doi.org/10.1127/0372-8854/2012/S-00075.

Zagórski, P., Frydrych, K., Jania, J., Błaszczyk, M., Sund, M., Moskalik, M., 2023. Surges in three svalbard glaciers derived from historic sources and geomorphic features. Ann. Am. Assoc. Geogr. 113 (8), 1835–1855. https://doi.org/10.1080/24694452.2023.2200487.

Zhang, X., Flato, G., Kirchmeier-Young, M., Vincent, L., Wan, H., Wang, X., et al., 2019. 'Changes in temperature and precipitation across Canada' in eds E. Bush, and D. S. Lemmen (Ottawa, ON: Canada's changing climate Report. Government of Canada), 112–193. https://doi.org/10.4095/327811.